Title

The functions of SIRT7 in the maintenance of neural stem cells and the regulation of the somatotroph axis

Author

OHKUBO, RIKA

Publication Date

2019

Peer reviewed|Thesis/dissertation

The functions of SIRT7 in the maintenance of neural stem cells and the regulation of the somatotroph axis

By

Rika Ohkubo

A dissertation submitted in partial satisfaction of the
requirement for the degree of
Doctor of Philosophy
in
Metabolic Biology
in the
Graduate Division
of the
University of California, Berkeley

Committee in charge:

Professor Danica Chen, Chair
Professor David Schaffer
Professor Sona Kang
Professor Jen Chywan Wang

Fall 2019

The functions of SIRT7 in the maintenance of neural stem cells
and the regulation of the somatotroph axis

By Rika Ohkubo

Abstract

The functions of SIRT7 in the maintenance of neural stem cells
and the regulation of the somatotroph axis

by

Rika Ohkubo

Doctor of Philosophy in Metabolic Biology

University of California, Berkeley

Professor Danica Chen, Chair

SIRT7 is a histone deacetylase that represses the expression of ribosomal proteins and mitochondrial ribosomal proteins to regulate the unfolded protein responses in the ER (UPR^{ER}) and the mitochondria (UPR^{mt}). At the organismal level, SIRT7 deficiency results in the development of fatty livers and compromised maintenance of hematopoietic stem cells. Using a SIRT7 knockout mouse model, I found that SIRT7 deficiency also leads to reduced number of neural stem cells and reduced neurogenesis, suggesting that the role of SIRT7 in stem cell maintenance is conserved across tissues. I also revealed hepatic gene expression changes and metabolic characterization of SIRT7 knockout mice that are consistent with the repression of the somatotroph axis, uncovering a physiological response to loss of proteostasis.

Table of contents

List of figures

Acknowledgements

I would like to thank my PhD advisor, Danica Chen. I am so lucky to have got a chance to join her lab and have got support from her. She was always encouraging especially when I faced with troubles. I learned not only science but also important things I should know to survive in a real life from her.

I also would like to thank all the current and past labmembers. Especially, Jenny and Hanzhi, who are my great ex-labmates, mentors and friends. We shared a lot of time inside the lab and outside the lab. Without them, my graduate student's life had been less memorable. They helped me by giving me intellectual input and emotional support even after they left the lab. Outside the lab, I don't remember how many times we went to "Great China" and Dim Sum places together. Chatting with great friends with good food helped me a lot to de-stress! Also, Wei, who is the biggest guinea pig lover I've ever seen, supported me in many ways. I especially have to thank her patient. She is the one who always listened my random complaints.

Lastly, I would like to thank my family. Dad and mom always supported me to get a great education, which encouraged me to get a PhD. My sister and her husband were my great supporters. Whenever I had to make a hard decision, they helped me to find a right way.

Chapter1. Introduction

Part1: An overview of neurogenesis during physiological aging, neural stem maintenance and age-associated cognitive dysfunctions

The increase in neurodegenerative diseases along with the increase in elderly population is emerging as a major concern. It is well known that the susceptibility of neurodegenerative diseases increases with age and is affected by genetic and environmental factors. The hallmarks of brain aging include increased oxidative stress, metabolic impairment, DNA damage, apoptosis, etc, all of which can exacerbate the development of neurodegenerative diseases [7]. Therefore, it is important to find interventions that slow the aging process to prevent age-associated cognitive dysfunctions and neurodegenerative diseases. It is well known that neurogenesis decreases with age and enhancing neurogenesis through exercise, caloric restriction or other interventions is beneficial to cognitive functions [8][9][10]. There are several hypotheses about decreased neurogenesis with age: increased quiescence of NSCs, depletion of neurogenesis due to the decreased NSC pool, depletion of neurogenesis due to the fate change and/or the increased neuronal death [10]. However, whether adult neurogenesis persists in rodents, non-human primates and humans are still under debate [11][12][13]. In this part, I review the function of NSC and the relationship between decreased neurogenesis and age-associated cognitive dysfunctions.

Adult neurogenesis in the mammalian brain and its function

It has been reported that adult neurogenesis occurs in only two regions in the mammalian brains: the subventricular zone (SVZ) of the lateral ventricles [14][15][16] and the subgranular zone (SGZ) of the dentate gyrus of the hippocampal formation [17][14].

NSCs and neural stem cell progenitor cells (NSPCs) from the SVZ migrate into the rostral migratory stream (RMS) to provide interneurons destinated for the olfactory bulb (OB) [18][19][20] and neurogenesis in the OB may be important for sensory discrimination. However, the debate on whether neurogenesis in the OB exists in the human brains is still ongoing [21] and the functions of neurogenesis in the OB remain unclear. In addition to neurogenesis in the OB, NSCs from the SVZ can migrate into lesions and differentiate into interneurons, astrocytes and oligodendrocytes [22][23][24][25]. These findings indicate that NSCs in the SVZ play a vital role in brain regeneration after injuries.

Newborn cells from the SGZ migrate into the granular layer of the dentate gyrus (DG) in the hippocampus, where most of them become excitatory granule cells, whose axons form the mossy fibers that link the DG to CA3 [26]. Adult neurogenesis in the hippocampus has attracted significant attention because the new neurons in the hippocampus may be beneficial to cognitive functions by increased plasticity and/or improved the connectivity with other neurons [27][28]. Exercise and caloric restriction are well known regimens to enhance neurogenesis in the DG and

improve cognitive functions [29][30]. NSC transplantation and infusions of young plasma can be also potential treatments for age-associated memory impairment and other neurodegenerative diseases such as Alzheimer's disease and Parkinson's disease [31][32][33]. Therefore, it will give us a great advantage to fully understand the mechanisms how the adult neurogenesis in the DG is regulated, and it will be therapeutically beneficial to find ways to manipulate the rate of adult neurogenesis.

The functions of NSCs

NSCs both in the SVZ and the SGZ have the capacity to self-renew and provide multiple neural lineages, including neurons, astrocytes and oligodendrocytes [34]. Although NSCs in the SVZ and the SGZ share some common characteristics and immunohistochemical markers, they also have different properties and markers due to the difference of their regional localizations in the brain.

In the SVZ, quiescent NSCs (quiescent Type B1 cells) express GLAST, GFAP, CD133 and Sox2. Once they are activated (active Type B1 cells), they start to express Nestin, EGFR and ASCL1. B1 cells can further give rise to neuroblasts (Type A cells) through transient amplifying cells (Type C cells). C cells still express EGFR and ASCL1 but do not express GFAP, GLAST CD133 or Nestin. On the other hand, A cells express doublecortin (Dcx) and eventually they become neurons [35][36][37].

In the SGZ, NSCs (Radial glia-like cells) express GFAP, Nestin, Sox2, and Ascl1, and have astrocytic features. Radial glia-like cells are generally quiescent, but they can provide astrocytes or neurons via more proliferating intermediate progenitor cells (IPCs), which are committed to the neuronal fate. IPCs lose GFAP, Nestin and Sox2 expressions and start to express the T-box brain protein 2 (Tbr2/Eomes) and Ki67. IPCs give rise to neuroblasts, which express Dcx and eventually mature into functional Prox1-positive dentate granule neurons [38].

In vitro, NSCs from both the SVZ and the SGZ can be cultured and generate neurospheres. The neurospheres can be expanded under serum-free medium supplemented with pleiotropic growth factors such as epidermal growth factor (EGF) and basic fibroblast growth factor (FGF2) without losing their self-renewal potential and multipotency [39]. Interestingly when pleiotropic growth factors are removed and serum is added to the medium, the neurospheres can differentiate into neurons, astrocytes and oligodendrocytes [40]. Therefore, the cellular components of NSC niches and the factors the niche cells provide such as cytokines and growth factors seem to affect the self-renewal potential and the fate of differentiation of NSCs.

The maintenance and regulation of neural stem cells

The self-renewal and the differentiation fate of NSCs are regulated by extrinsic factors such as neurotransmitters, signaling pathways, growth factors and neurotrophic factors, and intrinsic factors such as transcriptional factors, microRNA and epigenetic regulation [41]. Here I will

focus on the roles of two important signaling pathways, Notch signaling pathway and Wnt signaling pathway, and the functions of growth factor/cytokine.

Notch signaling pathway

Notch signaling pathway is one of the most famous intracellular signaling pathway and important for multiple cell differentiation processes during embryonic and adult life [42], the normal development of the nervous system [43][44], and also the regulation of HSCs [45][46][47]. Once a ligand from the adjacent cell binds to an extracellular Notch receptor, γ-secretase cleaves the NICD portion of the Notch receptor. The cleaved NICD is transported into the nucleus and activates the transcription of Notch target genes. Mammals have four Notch paralogues (Notch1–4), three Delta-like ligands (DLL1, DLL3 and DLL4) and two Jagged ligands (JAG1 and JAG2) [48]. Notch signaling pathway is particularly important for the self-renewal of NSCs and the maintenance of undifferentiated NSCs. It has been shown that Notch signaling pathway is required for the long-term maintenance of NSCs and the inhibition of Notch signaling pathway causes the premature neural differentiation and the depletion of NSCs [49][50]. In addition to the maintenance of NSCs, Notch signaling pathway plays a role in the determination of NSC cell fate. It is known that Notch signaling pathway promotes gliogenesis and inhibits neurogenesis by inhibiting the expressions of proneural genes such as Mash1 and Ngn1 [51][52]. These findings indicate the requirement of Notch signaling for the maintenance of NSCs and the proper control of NCS cell fate decisions.

Wnt signaling pathway

Wnt signaling pathway is important for the regulation of embryonic development and tissue homeostasis. Wnt signaling pathway consists of two pathways: a canonical pathway (Wnt/β-catenin) and a non-canonical pathway (β-catenin independent pathway). Wnt proteins are secreted glycosylated proteins and bind to the Frizzled (Fz) receptor family. In the canonical pathway, when Wnt is not bound to the Fz receptor, cytoplasmic β-catenin forms a complex with APC, Axin, CKI and GSK3. β-catenin is phosphorylated by CKI followed by GSK3 and the phosphorylated β-catenin is ubiquitinated by the E3 ubiquitin ligase β-Trcp, which targets β-catenin for proteosomal degradation. In the presence of Wnt, Wnt binds to the Fz and its co-receptor lipoprotein receptor-related protein (LRP) 5/6, which promotes the recruitment of Dvl and Axin. This prevents β-catenin from proteosomal degradation. The accumulated β-catenin in cytosol is translocated into the nucleus, where it works as a co-activator for TCF to activate Wnt responsive genes [53][54][55]. In the non-canonical pathway, the pathway is independent of β-catenin. In the non-canonical pathway, Wnt stimulates small GTPases of the Rho family to control tissue polarity, cytoskeletal reorganization and cell movement, or acts via heterotrimeric G proteins to control Ca2+ signaling [56]. A numerous number of Wnt lignd knockout mouse models are available. Their phonotypes vary one from another but most of them show impaired neurogenesis [57]. These mouse models clearly show the importance of Wnt signaling pathway in neurogenesis, and it has been suggested that both the canonical and non-canonical signaling pathways have multiple roles during developmental stages to adult neurogenesis [58]. Wnt-3a, a canonical Wnt ligand, is a key regulator of adult neurogenesis and overexpression of Wnt-3a is sufficient to increase neurogenesis in the hippocampus [59]. Wnt-3a is secreted by astrocytes and

the number of Wnt-3a secreting astrocytes declines during aging [60], which may cause decreased neurogenesis with age. On the other hand, Wnt-5a and Wnt-7a, which are non-canonical Wnt ligands, regulate the morphology of dendric spines. Wnt-5a increases dendric spine morphogenesis [61] and Wnt-7a similarly increases the density and maturity of dendric spines [62]. These findings indicate that Wnt signaling has to be properly controlled for the normal development of the nerve system and the maintenance of adult neurogenesis.

Growth factor/Cytokine

FGFs and EGF are known to act as mitogens for NSCs in vivo and in vitro, and these growth factors are important to maintain the self-renewal and multilineage potential of NSCs [63][64]. It is also suggested that IGF-1 involves in the maintenance of NSCs working with FGFs and EGF [65]. In respect of cell fate determination and cell differentiation, bone morphogenetic proteins (BMPs) are regarded as critical regulators. BMPs promote the differentiation of NSCs into astrocytes and prevent them from differentiating into oligodendrocytes [66][67]. Additionally, Interleukin (IL)-6 acts for astrocyte differentiation in synergy with BMPs [68]. On the other hand, Brain-derived neurotrophic factor (BDNF) is known to promote neurogenesis [69][70][71].

Impaired neurogenesis during aging

It is well known that neurogenesis decreases with age, which may cause cognitive dysfunctions. There are mainly four potential causes of decreased neurogenesis during aging: 1) Depletion of NSC pool 2) increased quiescent NSCs and decreased proliferation of NSPCs 3) cell fate change, and 4) increased death of newborn neurons [10]. A lot of studies showed that the number of Nestin and Sox2+ NSPCs in the hippocampus greatly decreases with age [72][73], and the decreased number of NSPCs causes overall reduction in the rate of neurogenesis. In addition to the decreased number of NSCs, the decreased neurogenesis is accelerated by the increased qNSCs and the decreased proliferation of NSPCs [74]. Little is known about the mechanisms underlying the activation of NSCs and the reasons that the activation of NSCs becomes less with age. Protein aggregation in NSCs and the inflammatory microenvironment have been postulated as causes of NSC inactivation. A previous study showed that active NSCs had active proteasome, while quiescent NSCs had protein accumulation and enlarged lysosome, and quiescent NSCs in aged mice showed defects in the lysosome [75]. The enhancement of aggregated protein clearance through the lysosome pathway in aged quiescent NSCs ameliorates the ability of quiescent NSCs to be activated. Not only the cell autonomous changes with age, the change of microenvironment with age also has to be considered because the microenvironment greatly changes during aging and becomes more inflammatory [76]. There are many researches that showed direct or indirect effects of inflammation on neurogenesis and the blockade of inflammation can improve decreased neurogenesis with age [77][72][78]. Inflammation also affects both the fate of NSCs and the survival of newborn neurons [79]. For example, IL-1β, a pro-inflammatory cytokine, preferentially shifts the fate of NSPCs toward astrocytes [80]. On the other hand, LPS, a potent activator of microglia, decreases the survival of cells differentiated from NSCs in vitro, which decreases neurogenesis [81]. Taken together, interventions which relieve inflammation in the brain such as caloric restriction and metformin treatment, seem attractive ways to improve age-associated cognitive dysfunctions. However, it is still valuable to

pursue the mechanisms how NSC activation, proliferation and differentiation are regulated more deeply to expand the potential therapeutic regimens to maintain brain health during aging. Obviously, the balance between active NSCs and quiescent NSCs has to be properly maintained to prevent the early depletion of NSCs as well as their differentiation fates to prevent brain cancers including astrocytomas and oligodendrogliomas.

Part2: An overview of the regulation of GH/IGF-1 signaling pathway during physiological aging

Physiologically, the GH/IGF-1 signaling is known to promote growth and the suppression of GH/IGF-1 signaling has been observed in aged animals and progeroid [5][6]. On the other hand, attenuated GH/IGF-1 signaling has been shown to extend lifespan in worms, flies and mice [82]. Therefore, it is likely that the suppression of GH/IGF-1 signaling works as a protection against a variety of stress and damages during aging. However, the mechanism of age-associated suppression of GH/IGF-1 signaling is largely unknown. In this part, I review the roles of GH/IGF-1 signaling in lifespan and the potential causes of the decreased GH/IGF-1 signaling pathway.

The roles of GH signaling pathway against aging and stress

GH is a peptide hormone secreted from the anterior pituitary gland and acts on many tissues. Throughout the life, GH stimulates protein production, promotes the utilization of fat, inhibits the action of insulin, and raises blood glucose level. GH also raises the level of IGF-1. During childhood and adolescence, GH is particularly important for the growth of bones and cartilage [83]. The secretion of GH peaks during puberty and its secretion gradually declines with age after the puberty. It has been shown that GH or GH receptor (GHR) deficient mice have an extended lifespan [84]. Not only aging, a variety of stress also suppress the GH secretion. Under stressed conditions, the shift of the metabolism to a catabolic state from an anabolic state happens to cope with the stress by exerting available energy resources [85]. This shift causes the decreased secretion of GH by cortisol and the inhibition of GH by glucocorticoids. Since the suppression of GH leads to enhanced insulin sensitivity, increased utilization of lipids and decreased inflammation [83], the suppression of GH signaling pathway may be an attractive approach to treat or prevent aging associated diseases such as cancers and diabetes.

The roles of IGF-1 signaling pathway against aging and stress

Similar to GH, the level of IGF-1 decreases with age and under the stressed conditions since IGF-1 secretion is positively regulated by GH [86]. IGF-1 is a peptide hormone mainly produced in the liver. The main functions of IGF-1 are the promotion of muscle, bone and tissue growth, and the regulation of blood glucose level [87]. In contrast to the functions of GH, IGF-1 lowers the blood glucose level by controlling carbohydrate metabolism and glycogen synthesis [88]. Caloric restriction is known to suppress IGF-1 and insulin levels, which leads to increased insulin sensitivity, enhanced resistant to stress and reduced cancer risks [89]. Although it has been shown that the downregulation of IGF-1 signaling pathway causes the extension of lifespan from worms to mice [82], the effects in human still remain unclear [90][91]. Recently a study has suggested that the low circulating IGF-1level can be used to predict life expectancies in humans with exceptional longevity [92], and it seems the inhibition of IGF-1 signaling pathway attracts more and more attention as a therapeutic use. However, the low IGF-1level can bring negative impacts on the maintenance of bone mass, muscle mass and brain functions [93][94]. Therefore, we still do not know whether the inhibition of IGF-1 signaling pathway is beneficial to humans.

What we can say with confidence is that we should maintain the optimal level of IGF-1 throughout life but not excessively low or high IGF-1 levels.

Chapter 2. Neural stem cell maintenance by SIRT7

Introduction

The silent information regulator (SIR) genes (Sirtuins), the mammalian homologs of the yeast Sir2, comprise a highly conserved family of proteins, with one or more sirtuins present in virtually all species from bacteria to mammals. In mammals, seven Sirtuin genes (SIRT1-SIRT7) have been identified. From the fact that the enzymatic reaction catalyzed by Sirtuins requires NAD+ as a substrate, we can speculate that sirtuins are heavily involved in cellular metabolic pathways.

Our lab has previously demonstrated that SIRT7 interacts with nuclear respiratory factor 1 (NRF1), a master regulator of mitochondria, at the proximal promoters of mitochondrial ribosomal proteins (mRPs) and mitochondrial translation factors (mTFs), and suppresses mitochondrial activity and proliferation in HSCs [3]. To prevent the depletion of HSCs, it is important to precisely regulate the activation of HSCs. The study has demonstrated that SIRT7 inactivation causes reduced quiescence in HSCs and increased mitochondrial protein folding stress. Also, it has been demonstrated that the expression of SIRT7 decreases in HSCs from old mice compare to young mice. From this study, it is clear that SIRT7 plays a vital role in regulating the HSC homeostasis and controlling the mitochondrial activity in HSCs. Numerous diseases are associated with mitochondrial dysfunction and failure of protein folding such as spastic paraplegia, Parkinson's disease, Friedreich's ataxia and cancer. Therefore, it would be interesting to investigate if SIRT7 is also critical in the regulation of mitochondrial biogenesis in NSCs and the maintenance of NSCs.

Here, we show that the knockout of SIRT7 caused cognitive impairment in young mice compared to wild-type mice (WT) and the overexpression of SIRT7 in the DGs of aged mice improved cognitive functions by enhancing neurogenesis. This study will shed light on the new roles of SIRT7 in the brain and provide a better understating of the maintenance of NSC homeostasis.

Results

SIRT7 deficient mice have a decreased NSC pool size and neurogenesis

To investigate whether the deficiency of SIRT7 in the brain causes adverse effects on the functions of NSCs, we checked the proliferation of NSCs, the number of NSPCs and the number of newborn neurons. Interestingly, we found that the proliferation of NSCs greatly decreased in the brains of SIRT7 KO mice compared to WT control mice by 1-day BrdU staining (Fig.1A and 1B). Sox2 staining and 4-weeks BrdU staining showed the decreased proliferation and/or decreased survival of NSPCs (Fig.1C), the decreased number of NSPCs (Fig. 1D) and the decrease of overall neurogenesis in SIRT7 KO mice (Fig. 1E). These data suggest that SIRT7 KO mice have less activated NSPCs than WT control mice, which causes decreased neurogenesis. Taken together, SIRT7 plays important roles in the maintenance of NSPC pool and the regulation of NSPC proliferation.

SIRT7 deficient mice show spatial memory decline

Decreased neurogenesis is often correlated with cognitive impairment [32]. Therefore, we decided to investigate whether SIRT7 KO mice have impaired cognitive function compared to WT control mice using Morris Water Maze (MWM). MWM is a behavioral procedure widely used to assess spatial memory [95]. SIRT7 KO mice showed slower spatial learning and higher cumulative search error (CSE) than WT control mice (Fig. 2A, 2B). We conducted a probe test to assess reference memory 24 hours after the 5-days training. Interestingly, SIRT7 KO mice spent more time to reach the place where the platform was located during the training period compared to WT control mice in 24hr probe test (Fig. 2D) and did not show preference to the target quadrant while WT control mice showed the preference (Fig. 2F). Additionally, the proximity of SIRT7 KO mice to the platform was not as close as the proximity of WT control mice (Fig.2H). SIRT7 KO mice crossed the previous platform location (Fig. 2G), indicating that SIRT7 KO mice showed weaker spatial reference memory than WT control but SIRT7 KO mice still retained the spatial reference memory 24 hours after the training. During the 5-days training and the probe test, there was no difference in the swim speed between WT control and SIRT7 KO mice (Fig. 2C and 2E). Taken together, these data showed that SIRT7 deficiency causes the impairment of spatial memory learning and retention.

Discussion

In this study, we uncovered the new roles of SIRT7 in NSCs and demonstrated that SIRT7 is involved in the maintenance of NSC homeostasis. Interestingly we revealed that the deletion of SIRT7 in the brain causes the decreased neurogenesis due to the decreased number of NSPCs and the decreased NSPC proliferation. From these findings, we can assume that SIRT7 is essential to activate NSCs and let them enter the cell cycle and proliferate. The loss of SIRT7 leads to increased ER stress [4] in the liver and mitochondria stress [3] in HSCs, and both stress can inhibit protein translation. It remains unclear how SIRT7 controls the activation and the proliferation of NSCs, but the suppression of protein translation due to the increased ER stress and mitochondria stress may be the causes of the decreased activation and proliferation of NSCs.

SIRT7 KO mice showed worse spatial memory than WT control mice in MWM, which can be explained by the decreased neurogenesis in SIRT7 KO mice.

Caloric restriction is known to activate sirtuins and an attractive regiment to give great health benefits including improved cognitive functions [9]. We have not tested whether improved cognitive functions by caloric restriction depends on the roles of SIRT7. However, the results we showed in this research indicates the beneficial effects of caloric restriction on the cognitive functions may be partially through the activation of SIRT7.

The mechanism how SIRT7 regulates NSC homeostasis remains unclear and has to be uncovered. Fully understanding the function of SIRT7 in NSCs will give great insights to develop noble therapeutic methods to combat age-associated cognitive dysfunction and neurodegenerative diseases.

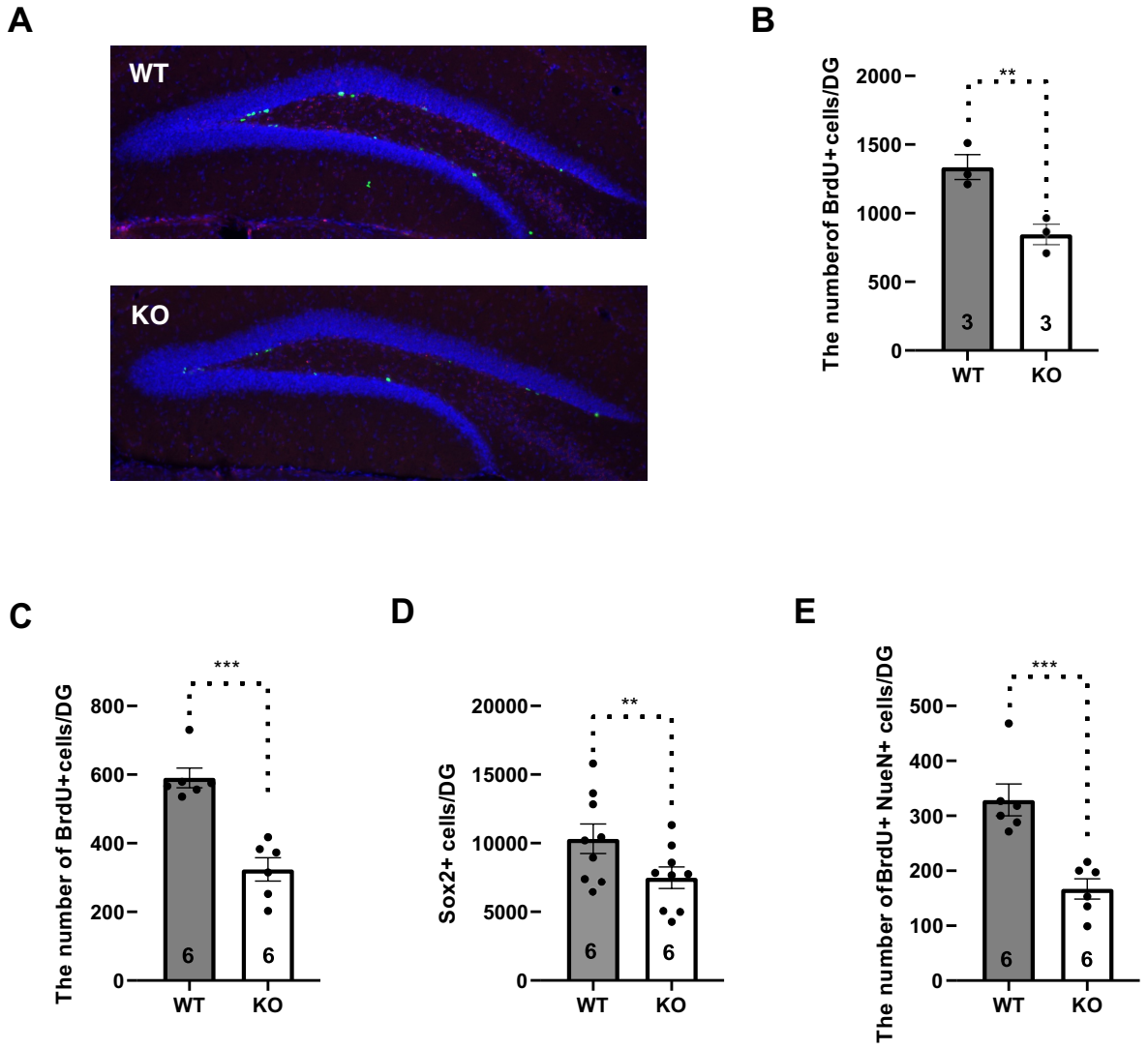

Figure 1. SIRT7 regulates the proliferation of NSCs and the loss of SIRT7 causes the decreased neurogenesis.

(A) 1-day BrdU experiment showing the decreased proliferation of NSPCs in SIRT7 KO mice compared to WT control mice.
(B) Quantification of the number of BrdU in 1-day BrdU experiment.
(C) Quantification of the number of BrdU positive cells in DG in 4 weeks BrdU experiment showing the decreased proliferating NSPCs in SIRT7 KO mice compared to WT control mice.
(D) Quantification of the number of Sox2 positive cells in DG showing the decreased number of NSPCs in SIRT7 KO mice compared to WT control mice.
(E) Quantification of the number of BrdU/NeuN double positive cells in DG in 4 weeks BrdU experiment showing the decreased neurogenesis in SIRT7 KO mice compared to WT control mice.

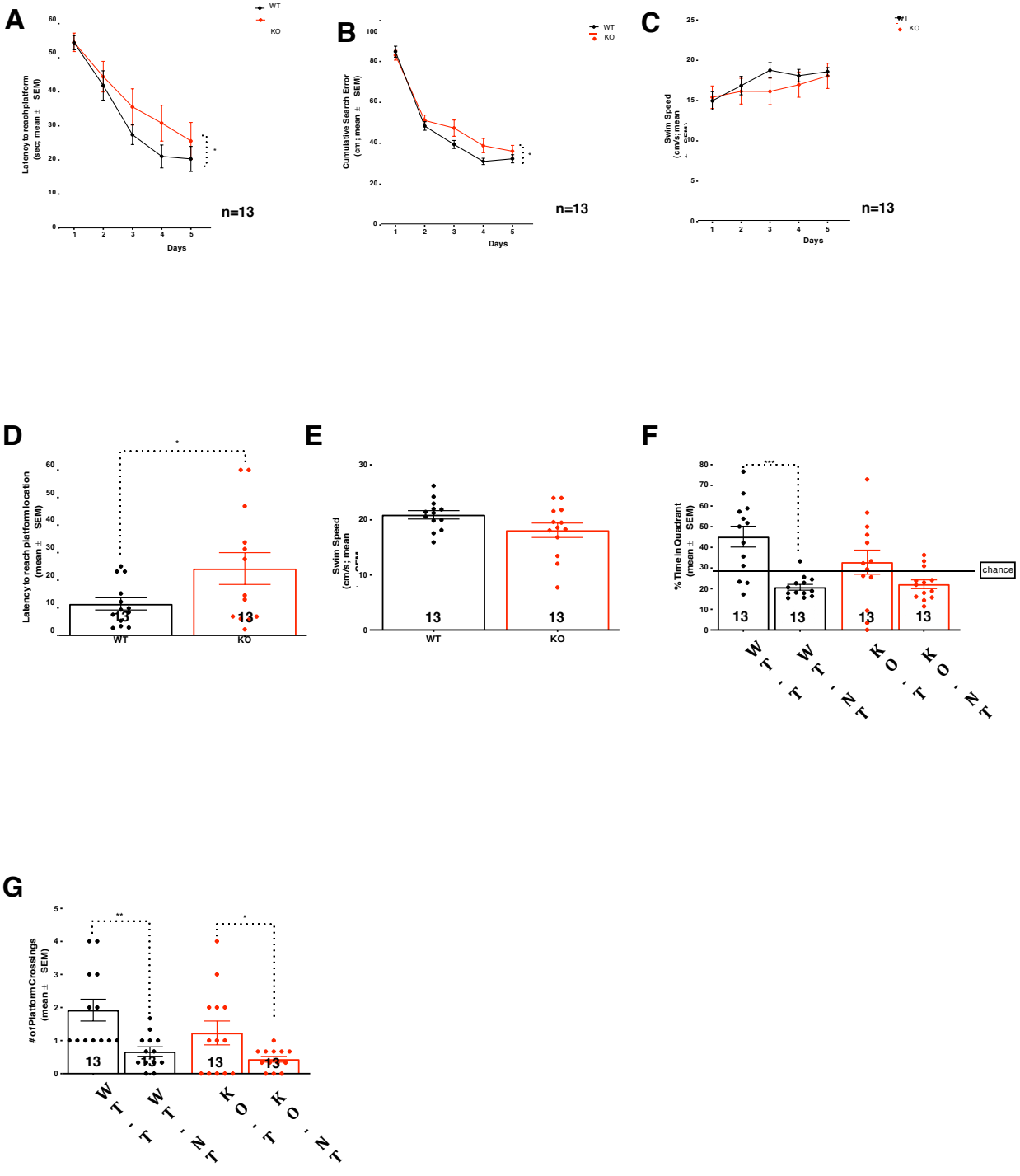
A
WT
KO
Latency to reach platform (sec; mean ± SEM)
Days
n=13
B
WT
KO
Cumulative Search Error (cm; mean ± SEM)
Days
n=13
C
WT
KO
Swim Speed (cm/s; mean
Days
n=13
D
Latency to reach platform location (mean ± SEM)
13
13
WT
KO
E
Swim Speed (cm/s; mean
13
13
WT
KO
F
% Time in Quadrant (mean ± SEM)
chance
13
13
13
13
WT, T
WT, NT
KO, T
KO, NT
G
# of Platform Crossings (mean ± SEM)
13
13
13
13
WT, T
WT, NT
KO, T
KO, NT

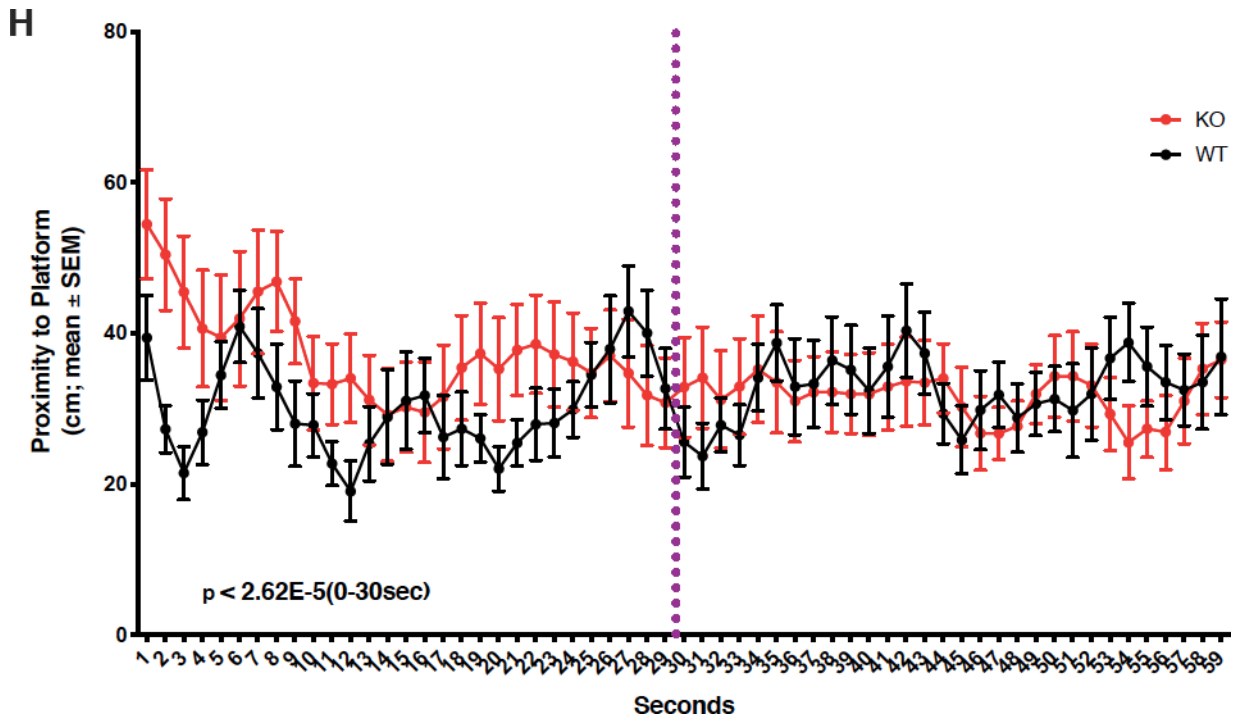

Figure 2. MWM showed the deletion of SIRT7 causes the impairment of spatial memory.

(A) Latency to reach the platform during the 5-days training showing slower spatial learning in SIRT7 KO mice than WT control mice.
(B) CSE to reach the platform during the 5-days training showing slower spatial learning in SIRT7 KO mice than WT control mice.
(C) Swim speed during the 5-days training.
(D) Latency to reach the platform during the 24hr probe showing weaker spatial reference memory in SIRT7 KO mice than WT control mice.
(E) Swim speed during the 24hr probe.
(F) Preference in the target quadrant during the first 30 seconds of the 24hr probe showing the weaker spatial reference memory in SIRT7 KO mice than WT control mice.
(G) The number of crossing of the platform location during the first 30 seconds of the 24hr probe.
(H) Proximity to the platform location during the 24hr probe.

Chapter3. The role of SIRT7 in the regulation of GH/IGF-1 signaling pathway through proteostasis

Introduction

It has been known that the GH/IGF-1 signaling pathway is downregulated by aging and a variety of stress, which suggests that the downregulation of GH/IGF-1 signaling pathway works as a protective program by switching from growth and proliferation to the protection and maintenance of tissues [91]. Although some studies showed that DNA damage causes the suppression of the GH/IGF-1 signaling pathway [6][96], it is not clear whether other kinds of stress can also cause the suppression of the GH/IGF-1 signaling pathway such as endoplasmic reticulum (ER) stress.

SIRT7 is highly expressed in the liver and our previous study found that SIRT7 binds to the transcription factor Myc, which is a master regulator of protein translation, and alleviates ER stress by suppressing Myc-dependent protein translation [4]. Importantly, SIRT7-deficient mice develop hepatosteatosis resembling human fatty liver disease induced by ER stress, and SIRT7 can attenuate high-fat diet-induced ER stress and the development of fatty liver disease in mice.

It has been shown that the total levels of ER proteins, including protein chaperones and folding enzymes decrease with age [97]. Compromised proper protein folding and the adaptive response of the UPR lead to the accumulation and the aggregation of misfolded proteins, which eventually causes ER stress. Some aging associated diseases including Alzheimer's diseases and Parkinson's disease can be explained by the failure of protein homeostasis and the increased ER stress with age.

In this study, we conducted Affymetrix microarray analysis to determine the gene expression changes in the liver caused by SIRT7 deletion. Interestingly, we found that the loss of SIRT7 causes the downregulation of the GH/IGF-1 signaling pathway through the activation of ER stress and this downregulation of the GH/IGF-1 signaling pathway can be partially reversed by the knockdown of Myc or ATF3, a member of the CREB family of basic leucine zipper transcription factors. These data indicate that ER stress causes the suppression of the GH/IGF-1 signaling pathway. Additionally, this study supports the idea that the suppression of the GH/IGF-1 signaling pathway works for cellular protection and may be beneficial to patients with aging associated diseases.

Results

Analysis of a microarray experiment showed that the GH/IGF-1 signaling pathway was dysregulated by the loss of SIRT7

To investigate the changes of gene expression by the deletion of SIRT7 in the mouse liver, we conducted Affymetrix microarray. The microarray analysis revealed 983 genes with significant changed expression in SIRT7 KO livers compared to the WT control livers (Benjamini-Hochberg FDR of 15%; Table 1). Among the differentially expressed genes, 440 genes were upregulated, and 543 genes were downregulated in the livers of SIRT7 KO mice. Gene ontology analysis revealed changes in inflammatory response, immune response and protein metabolism, which is consistent with the phenotype of SIRT7 KO mice [3][4][98].

Interestingly, we found that several genes related to the GH/IGF-1 signaling pathway were differentially expressed in SIRT7 KO livers compared to WT control livers including IGF binding proteins (IGFBPs), and receptors for growth hormones and growth factors (Table. 2). These gene expression changes were confirmed by qPCR (Figure. 3A-F). IGFBPs serve as carrier proteins for IGF-1. It is known that IGFBP1 is negatively and IGFBP3 is positively correlated with the IGF-1 level [99]. Therefore, the upregulation of IGFBP1 and the downregulation of IGFBP3 in the livers of SIRT7 KO mice indicate the decreased IGF-1 level in SIRT7 KO mice. Similarly, the downregulations of GhR, Epidermal Growth Factor Receptor (EGFR) and Fibroblast Growth Factor 1(FGF1) suggest that a variety of signaling pathways related to growth are suppressed in SIRT7 KO mice. These gene expression changes can explain the post-natal growth retardation of SIRT7 KO mice compared to the WT control mice [4][100].

To further confirm that the GH/IGF-1 signaling pathway is downregulated in the livers of SIRT7 KO mice, we measured the plasma IGF-1 level (Figure. 3G). Strickingly, SIRT7 KO mice had a significantly lower plasma IGF-1 level. Taken together, these data support that the GH/IGF-1 signaling pathway is downregulated by the loss of SIRT7.

The loss of proteostasis by the deletion of SIRT7 induce the dysregulation of the GH/IGF-1 signaling pathway

We investigated whether ER stress affects the activities of the GH/IGF-1 signaling pathway. SIRT7 is essential for the maintenance of proteostasis by inhibiting Myc and the loss of SIRT7 induces ER stress [4]. The increased ER stress in the liver of SIRT7 KO mice was confirmed by the increased phosphorylation level of eIF2a, and the suppressed insulin signaling pathway was confirmed by the decreased phosphorylation level of Akt (Fig. 4A). The increased ER stress were partially rescued by Myc knockdown (Fig. 4A). Intriguingly, Myc knockdown reversed the changes in gene expressions related to the GH/IGF-1 signaling pathway caused by the deletion of SIRT7 (Fig. 4B-F), which suggests the relief of ER stress reactivates the GH/IGF-1 signaling pathway. The reactivation of the GH/IGF-1 signaling pathway was additionally confirmed by the increased plasma IGF-1 level by Myc knockdown (Fig. 4G). The reactivation of the GH/IGF-1 signaling pathway by Myc knockdown indicates that the loss of proteostasis may suppress the GH/IGF-1 signaling pathway.

ATF3 expression induced by ER stress disturbs the GH/IGF-1 signaling pathway

Finally, we explored the mechanism which disturbs the regulation of the GH/IGF-1 signaling pathway upon ER stress. Several transcription factors which belong to ATF/CREB family are known to be activated by ER stress and mitochondrial stress [101][102]. ATF4 and ATF6 induces gene expressions involved in amino acid metabolism and the resistance to oxidative stress upon ER stress [103]. On the other hand, ATF5 relieves mitochondrial stress [104]. We found that ATF3 was upregulated in the livers of SIRT7 KO mice compared to WT control mice from the microarray analysis (Table 1). Similar to ATF4 and ATF5, ATF3 is also induced by ER stress and causes cell apoptosis [105]. We further investigated what genes are targeted by theses ATF proteins using Harmonizome web portal, which is a collection of processed datasets to mine information related to genes and proteins. Interestingly, ChIP sequencing data revealed that ATF3 binds to the promotor or the enhancer regions of a number of IGF-related genes (Table.3). In contrast, ATF4, ATF5, or ATF6 does not bind to the promotor or the enhancer regions of the IGF-related genes. Therefore, we decided to focus on the role of ATF3. The upregulation of ATF3 in the livers of SIRT7 KO mice was confirmed by qPCR and the expression of ATF3 was reversed by Myc knockdown and ATF3 knockdown (Fig. 5A). The gene expressions of some genes related to the GH/IGF-1 signaling pathway were reversed by hepatic ATF3 knockdown (Fig. 5B-E). To further validate that the inactivation of ATF3 can reactivate the downregulated GH/IGF-1 signaling pathway by the deletion of SIRT7, we measured the plasma IGF-1 level and the phosphorylation level of Akt. Intriguingly, the inactivation of ATF3 increased the plasma IGF-1 level (Fig. 5F) and the phosphorylation level of Akt in the livers of SIRT7 KO mice (Fig. 5G). Taken together, these data indicate that ATF3 inactivation can restore the normal GH/IGF-1 signaling.

Discussion

We found that the loss of SIRT7 causes the dysregulation of the GH/IGF-1 signaling pathway. The GH/IGF-1 signaling pathway declines with age [6] as well as with some stress such DNA damage [96]. In this research, we first showed that ER stress causes the downregulation of the GH/IGF-1 signaling pathway, and the GH/IGF-1 signaling pathway can be reactivated by the relief of ER stress vis the suppression of Myc or ATF3 in SIRT7 KO mice. ATF3 is a transcription factor which is activated by ER stress and is known to promotes apoptosis [105]. We revealed that ATF3 binds to the promotor or the enhancer regions of a number of IGF-related genes using ChIP sequencing data in Harmonizome web portal, which supports the idea that ATF3 is an important regulator of the GH/IGF-1 signaling pathway upon ER stress. Collectively, these results indicate that the suppression of the GH/IGF-1 signaling pathway works as a protective response to cellular stress. Our findings reinforce the potential use of the suppression of the GH/IGF-1 pathway to treat progeroid disorders and aging-associated diseases.

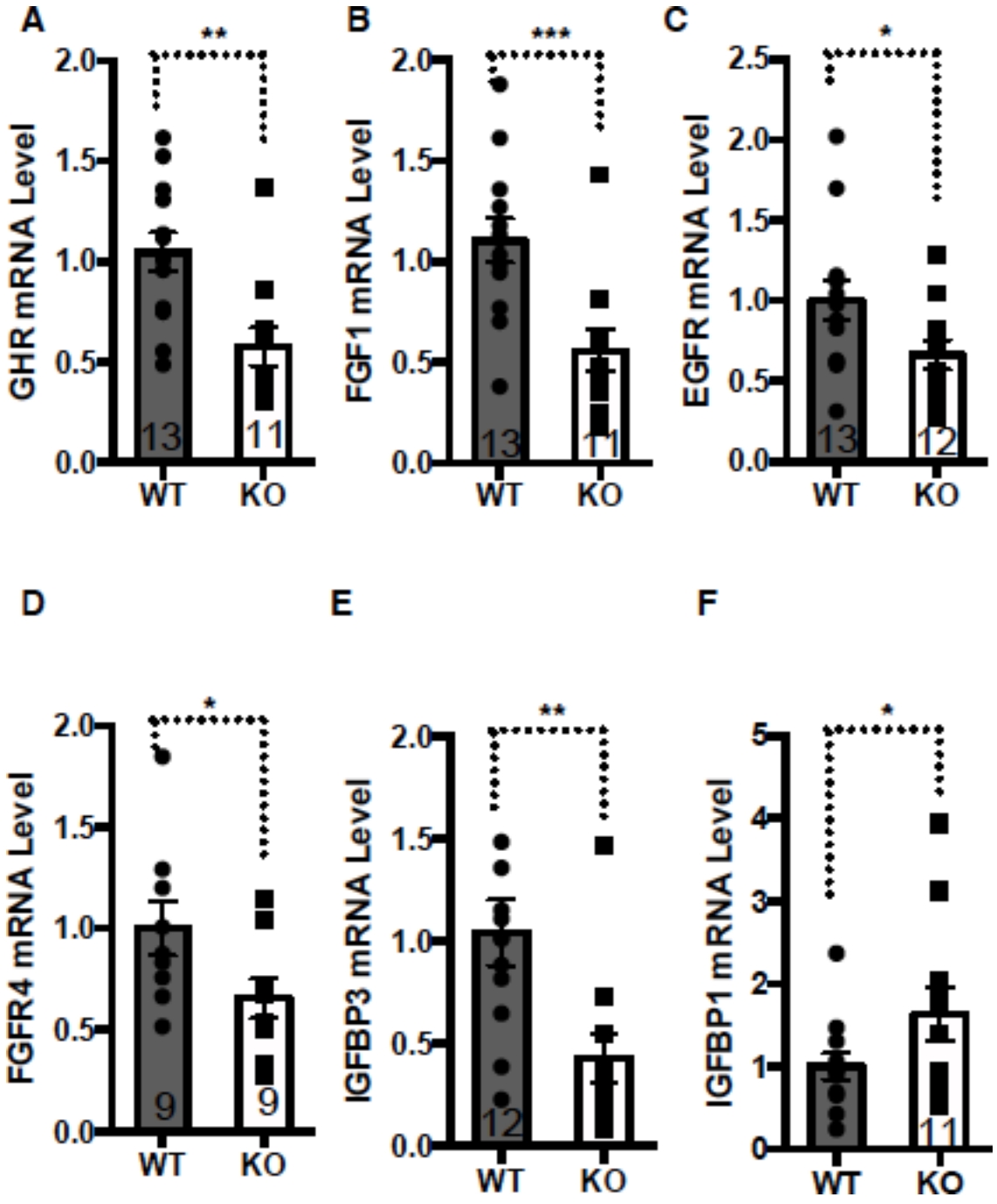
A
B
C
D
E
F
GHR mRNA Level
FGF1 mRNA Level
EGFR mRNA Level
FGFR4 mRNA Level
IGFBP3 mRNA Level
IGFBP1 mRNA Level
WT
KO
13
11
13
11
13
12
9
9
12
11
**
***
*
*
**
*

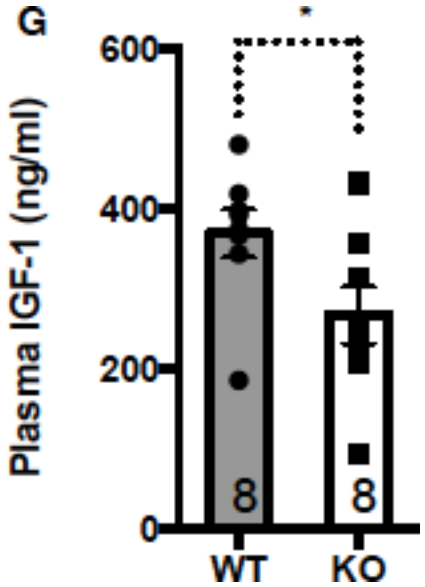

Figure 3. The deletion of SIRT7 in the liver causes the suppression of the GH/IGF-1 signaling pathway.

(A) – (F) Quantification of gene expression changed related to the GH/IGF-1 signaling pathway in the livers of SIRT7 KO mice compared to in the livers of WT control mice by qPCR showing the suppression of the GH/IGF-1 signaling pathway in the livers of SIRT7 KO mice

(G) Quantification of plasma IGF-1 levels by ELISA showing the lower plasma IGF-1 level in SIRT7 KO mice than WT control mice.

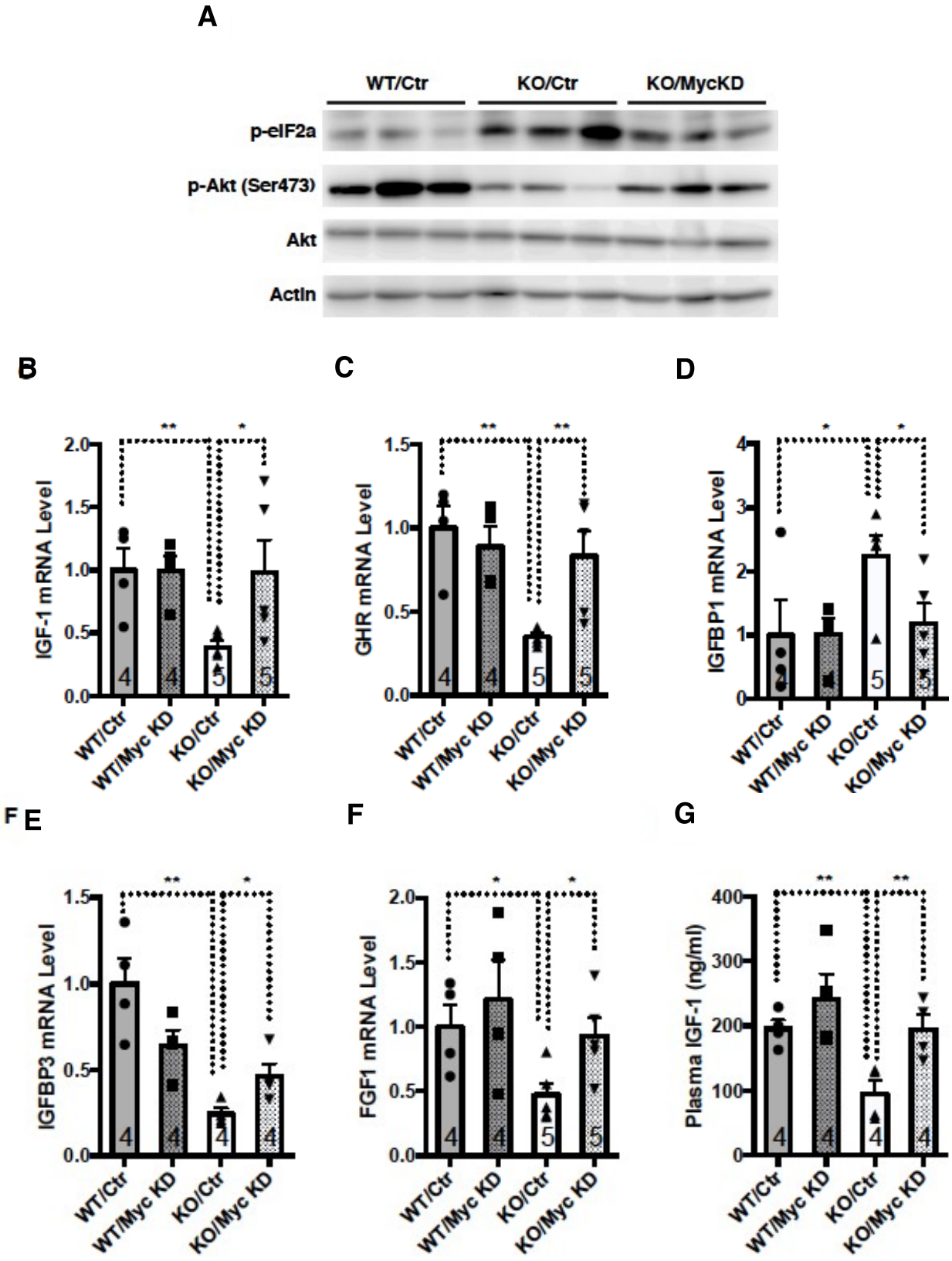
A
WT/Ctr
KO/Ctr
KO/MycKD
p-eIF2a
p-Akt (Ser473)
Akt
Actin
B
IGF-1 mRNA Level
C
GHR mRNA Level
D
IGFBP1 mRNA Level
F E
IGFBP3 mRNA Level
F
FGF1 mRNA Level
G
Plasma IGF-1 (ng/ml)
WT/Ctr
WT/Myc KD
KO/Ctr
KO/Myc KD

Fig 4. The accumulation of DNA damage and the loss of proteostasis by the deletion of SIRT7 suppress the GH/IGF-1 signaling pathway.

(A) Western analysis showing the inhibition of Myc relieves ER stresses and reverses the suppression of the GH/IGF-1 signaling pathway in the livers of SIRT7 KO mice.

(B) – (F) Quantification of gene expression changed related to the GH/IGF-1 signaling pathway in the livers of SIRT7 KO mice with Myc knockdown compared to in the livers of SIRT7 KO and WT control mice by qPCR showing the inhibition of Myc reverses the suppression of gene expressions related to the GH/IGF-1 signaling pathway.

(G) Quantification of plasma IGF-1 levels by ELISA showing the improved plasma IGF-1 level in SIRT7 KO mice with Myc knockdown compared to SIRT7 KO mice.

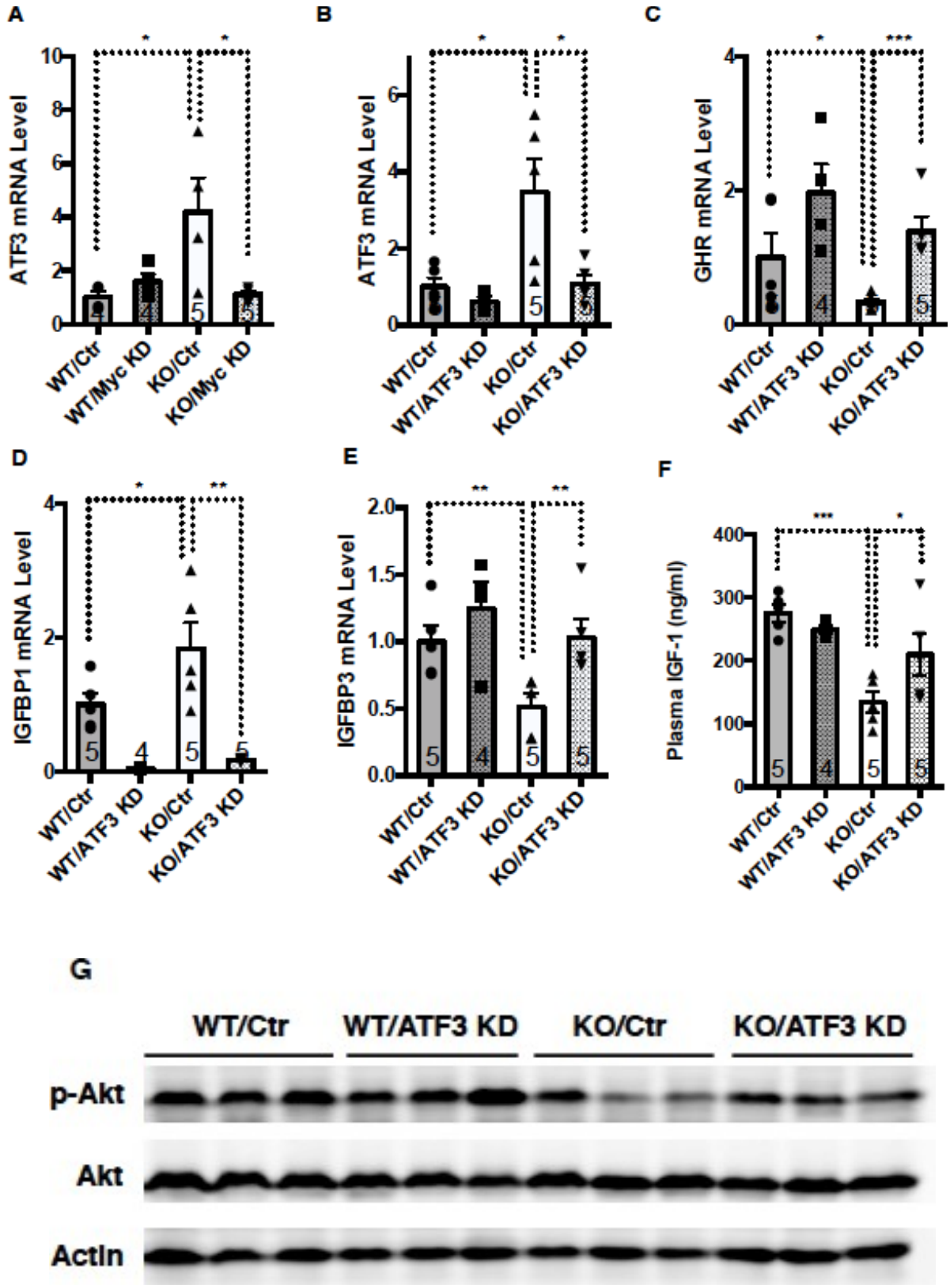
A
ATF3 mRNA Level
WT/Ctr
WT/Myc KD
KO/Ctr
KO/Myc KD
B
ATF3 mRNA Level
WT/Ctr
WT/ATF3 KD
KO/Ctr
KO/ATF3 KD
C
GHR mRNA Level
WT/Ctr
WT/ATF3 KD
KO/Ctr
KO/ATF3 KD
D
IGFBP1 mRNA Level
WT/Ctr
WT/ATF3 KD
KO/Ctr
KO/ATF3 KD
E
IGFBP3 mRNA Level
WT/Ctr
WT/ATF3 KD
KO/Ctr
KO/ATF3 KD
F
Plasma IGF-1 (ng/ml)
WT/Ctr
WT/ATF3 KD
KO/Ctr
KO/ATF3 KD
G
WT/Ctr
WT/ATF3 KD
KO/Ctr
KO/ATF3 KD
p-Akt
Akt
Actin

Fig 5. The suppression of ATF3 reverses the downregulated GH/IGF-1 signaling pathway by the deletion of SIRT7.

(A) Quantification of gene expression changes by qPCR showing the upregulated ATF3 gene expression in the livers of SIRT7 KO mice compared to WT control mice.

(B) – (E)Quantification of gene expression changes by qPCR showing the reactivation of the GH/IGF-1 signaling pathway by ATF3 knockdown in the livers of SIRT7 KO mice.

(F) Quantification of plasma IGF-1 levels by ELISA showing the improved plasma IGF-1 level by ATF3 knockdown in SIRT7 KO mice.

(G) Western analysis showing the inhibition of ATF3 reverses the suppression of the GH/IGF-1 signaling pathway in the livers of SIRT7 KO mice.

Code	Gene title	Symbol	Fold Change	p value
1420493_a_at	phosphate cytidylyltransferase 2, ethanolamine	Pcyt2	-4.483	0.000
1424238_at	sirtuin 7 (silent mating type information regulation 2, homolog) 7 (S. cerevisiae)	Sirt7	-4.211	0.000
1448741_at	solute carrier family 3, member 1	Slc3a1	-2.023	0.002
1455457_at	cytochrome P450, family 2, subfamily c, polypeptide 54	Cyp2c54	-1.908	0.001
1460258_at	leukocyte cell derived chemotaxin 1	Lect1	-1.784	0.000
1425127_at	hydroxy-delta-5-steroid dehydrogenase, 3 beta- and steroid delta-isomerase 2	Hsd3b2	-1.548	0.001
1434739_at	fragile X mental retardation 1 neighbor	Fmr1nb	-1.515	0.005
1450226_at	prolactin receptor	Prlr	-1.405	0.001
1421382_at	prolactin receptor	Prlr	-1.401	0.002
1419161_a_at	NADPH oxidase 4	Nox4	-1.164	0.001
1452416_at	interleukin 6 receptor, alpha	Il6ra	-1.154	0.000
1419510_at	carboxylesterase 1E	Ces1e	-1.112	0.005
1450725_s_at	carbonic anhydrase 14	Car14	-1.085	0.001
1451827_a_at	NADPH oxidase 4	Nox4	-1.070	0.003
1417765_a_at	amylase 1, salivary	Amy1	-1.061	0.000
1425853_s_at	prolactin receptor	Prlr	-1.042	0.004
1417600_at	solute carrier family 15 (H+/peptide transporter), member 2	Slc15a2	-1.037	0.002
1449248_at	chloride channel 2	Clcn2	-0.949	0.000
1449486_at	carboxylesterase 1G	Ces1g	-0.937	0.000
1451627_a_at	solute carrier family 1 (glial high affinity glutamate transporter), member 2	Slc1a2	-0.935	0.001
1449155_at	polymerase (RNA) III (DNA directed) polypeptide G	Polr3g	-0.910	0.000
1418596_at	fibroblast growth factor receptor 4	Fgfr4	-0.909	0.000
1443949_at	---	---	-0.891	0.001
1424958_at	carbonic anhydrase 8	Car8	-0.874	0.000
1421852_at	potassium channel, subfamily K, member 5	Kcnk5	-0.868	0.003
1419359_at	hexamethylene bis-acetamide inducible 1	Hexim1	-0.835	0.000
1450060_at	polymeric immunoglobulin receptor	Pigr	-0.823	0.000
1448927_at	potassium intermediate/small conductance calcium-activated channel, subfamily N, member 2	Kcnn2	-0.807	0.000
1418086_at	protein phosphatase 1, regulatory (inhibitor) subunit 14A	Ppp1r14a	-0.800	0.004
1455490_at	polymeric immunoglobulin receptor	Pigr	-0.798	0.000
1443695_at	hyaluronic acid binding protein 2	Habp2	-0.790	0.000
1418645_at	histidine ammonia lyase	Hal	-0.773	0.000
1449555_a_at	fetuin beta	Fetub	-0.765	0.003
1427711_a_at	carcinoembryonic antigen-related cell adhesion molecule 1	Ceacam1	-0.760	0.005
1420946_at	alpha thalassemia/mental retardation syndrome X-linked homolog (human)	Atrx	-0.757	0.000
1427008_at	ring finger protein 43	Rnf43	-0.738	0.001
1449001_at	isovaleryl coenzyme A dehydrogenase	Ivd	-0.734	0.002
1435405_at	SET domain containing 4	Setd4	-0.733	0.005
1431900_a_at	forkhead box A3	Foxa3	-0.724	0.001
1418940_at	sulfotransferase family 1B, member 1	Sult1b1	-0.721	0.002
1422826_at	insulin-like growth factor binding protein, acid labile subunit	Igfals	-0.720	0.000
1456377_x_at	LIM domain containing 2	Limd2	-0.719	0.004
1451579_at	cDNA sequence BC024139	BC024139	-0.716	0.000
1452079_s_at	DCN1, defective in cullin neddylation 1, domain containing 1 (S. cerevisiae)	Dcun1d1	-0.715	0.000
1452353_at	G protein-coupled receptor 155	Gpr155	-0.714	0.000
1424598_at	DEAD (Asp-Glu-Ala-Asp) box polypeptide 6	Ddx6	-0.706	0.000
1422812_at	chemokine (C-X-C motif) receptor 6	Cxcr6	-0.702	0.002
1416801_at	transient receptor potential cation channel, subfamily M, member 7	Trpm7	-0.697	0.000
1439422_a_at	family with sequence similarity 132, member A	Fam132a	-0.693	0.001
1417623_at	solute carrier family 12, member 2	Slc12a2	-0.691	0.006
1422168_a_at	brain derived neurotrophic factor	Bdnf	-0.688	0.003
1427371_at	ATP-binding cassette, sub-family A (ABC1), member 8a	Abca8a	-0.687	0.003
1426259_at	pantothenate kinase 3	Pank3	-0.681	0.001
1434620_s_at	family with sequence similarity 13, member B	Fam13b	-0.677	0.001
1431803_at	cytochrome P450, family 2, subfamily d, polypeptide 13	Cyp2d13	-0.675	0.000
1423136_at	fibroblast growth factor 1	Fgf1	-0.664	0.002
1434736_at	hepatic leukemia factor	Hlf	-0.663	0.003
1424576_s_at	cytochrome P450, family 2, subfamily c, polypeptide 44	Cyp2c44	-0.662	0.000
1424544_at	nuclear receptor binding protein 2	Nrbp2	-0.662	0.000
1426293_at	zinc finger protein 790	Zfp790	-0.662	0.000
1416258_at	thymidine kinase 1	Tk1	-0.661	0.001
1437614_x_at	zinc finger, DHHC domain containing 14	Zdhhc14	-0.660	0.001
1448555_at	RNA polymerase II associated protein 3	Rpap3	-0.659	0.003
1439167_at	peroxisomal trans-2-enoyl-CoA reductase	Pecr	-0.657	0.001
1425301_at	neural cell adhesion molecule 2	Ncam2	-0.655	0.002
1420913_at	solute carrier organic anion transporter family, member 2a1	Slco2a1	-0.653	0.001
1419321_at	coagulation factor VII	F7	-0.651	0.000
1427630_x_at	carcinoembryonic antigen-related cell adhesion molecule 1	Ceacam1	-0.649	0.000
1425596_at	expressed sequence AI317395	AI317395	-0.648	0.001
1427322_at	bromodomain and WD repeat domain containing 1	Brwd1	-0.646	0.001
1450494_x_at	carcinoembryonic antigen-related cell adhesion molecule 1	Ceacam1	-0.646	0.001
1460256_at	carbonic anhydrase 3	Car3	-0.641	0.001
1451760_s_at	RIKEN cDNA 2010001E11 gene /// expressed sequence AI317395	2010001E11Rik /// AI317395	-0.636	0.001
1424413_at	opioid growth factor receptor-like 1	Ogfrl1	-0.633	0.001
1460380_at	desmoglein 2	Dsg2	-0.626	0.003
1417841_at	peroxisomal membrane protein 2	Pxmp2	-0.623	0.001
1427191_at	natriuretic peptide receptor 2	Npr2	-0.619	0.001
1421733_a_at	protein-tyrosine sulfotransferase 1	Tpst1	-0.617	0.000
1425365_a_at	cytochrome P450, family 2, subfamily d, polypeptide 13	Cyp2d13	-0.616	0.000
1425675_s_at	carcinoembryonic antigen-related cell adhesion molecule 1	Ceacam1	-0.615	0.000
1425538_x_at	carcinoembryonic antigen-related cell adhesion molecule 1	Ceacam1	-0.609	0.000
1418050_at	glycosylphosphatidylinositol specific phospholipase D1	Gpld1	-0.609	0.001
1452294_at	protocadherin 1	Pcdh1	-0.608	0.000
1451857_a_at	notum pectinacetylesterase homolog (Drosophila)	Notum	-0.607	0.001
1425633_at	cDNA sequence BC026782	BC026782	-0.600	0.001
1426726_at	protein phosphatase 1, regulatory subunit 10 pseudogene /// protein phosphatase 1, regulatory subunit 10	Gm8801 /// Ppp1r10	-0.598	0.003
1431405_a_at	centrosome and spindle pole associated protein 1	Cspp1	-0.597	0.001

1426165_a_at	caspase 3	Casp3	-0.596	0.005
1434644_at	transducin (beta)-like 1 X-linked	Tbl1x	-0.592	0.001
1438975_x_at	zinc finger, DHHC domain containing 14	Zdhhc14	-0.587	0.002
1418858_at	aldehyde oxidase 3	Aox3	-0.587	0.002
1424312_at	adiponectin receptor 1	Adipor1	-0.583	0.001
1427561_a_at	afamin	Afm	-0.583	0.000
1436362_x_at	RIKEN cDNA 2700079J08 gene	2700079J08Rik	-0.580	0.000
1429122_a_at	RIKEN cDNA 1700040I03 gene	1700040I03Rik	-0.578	0.000
1419456_at	dicarbonyl L-xylulose reductase	Dcxr	-0.577	0.001
1422123_s_at	carcinoembryonic antigen-related cell adhesion molecule 1 /// carcinoembryonic antigen-related cell adhesion molecule 2	Ceacam1 /// Ceacam2	-0.572	0.004
1438069_a_at	RNA binding motif protein 5	Rbm5	-0.569	0.002
1420989_at	RIKEN cDNA 4933411K20 gene	4933411K20Rik	-0.567	0.000
1419747_at	asialoglycoprotein receptor 2	Asgr2	-0.566	0.000
1424861_at	RIKEN cDNA D930016D06 gene	D930016D06Rik	-0.565	0.000
1426727_s_at	protein phosphatase 1, regulatory subunit 10 pseudogene /// protein phosphatase 1, regulatory subunit 10	Gm8801 /// Ppp1r10	-0.562	0.004
1426597_s_at	intermediate filament family orphan 2	Iffo2	-0.555	0.005
1419173_at	aminoacylase 1	Acy1	-0.553	0.001
1417227_at	methylcrotonoyl-Coenzyme A carboxylase 1 (alpha)	Mccc1	-0.549	0.002
1448546_at	Ras association (RalGDS/AF-6) domain family member 3	Rassf3	-0.548	0.003
1422001_at	inhibin beta-C	Inhbc	-0.548	0.001
1452354_at	RIKEN cDNA 2810459M11 gene	2810459M11Rik	-0.547	0.000
1427482_a_at	carbonic anhydrase 8	Car8	-0.547	0.001
1440971_x_at	zinc finger protein 771	Zfp771	-0.546	0.000
1450715_at	cytochrome P450, family 1, subfamily a, polypeptide 2	Cyp1a2	-0.542	0.002
1425937_a_at	hexamethylene bis-acetamide inducible 1	Hexim1	-0.541	0.000
1422894_at	Scm-like with four mbt domains 1	Sfmbt1	-0.537	0.001
1438619_x_at	zinc finger, DHHC domain containing 14	Zdhhc14	-0.534	0.002
1425088_at	sodium channel, nonvoltage-gated 1 alpha	Scnn1a	-0.533	0.003
1417012_at	syndecan 2	Sdc2	-0.532	0.000
1450051_at	alpha thalassemia/mental retardation syndrome X-linked homolog (human)	Atrx	-0.530	0.000
1423571_at	sphingosine-1-phosphate receptor 1	S1pr1	-0.529	0.005
1450071_at	ash1 (absent, small, or homeotic)-like (Drosophila)	Ash1l	-0.529	0.000
1426574_a_at	adducin 3 (gamma)	Add3	-0.528	0.001
1427037_at	eukaryotic translation initiation factor 4, gamma 1	Eif4g1	-0.526	0.005
1421336_at	prospero-related homeobox 1	Prox1	-0.523	0.001
1448008_at	ankyrin repeat and KH domain containing 1	Ankhd1	-0.522	0.000
1418013_at	camello-like 1	Cml1	-0.520	0.001
1420390_s_at	zinc finger protein 354A	Zfp354a	-0.519	0.002
1429104_at	LIM domain containing 2	Limd2	-0.518	0.005
1425392_a_at	nuclear receptor subfamily 1, group I, member 3	Nr1i3	-0.516	0.006
1417406_at	SERTA domain containing 1	Sertad1	-0.515	0.004
1428045_a_at	E74-like factor 2	Elf2	-0.512	0.001
1424223_at	RIKEN cDNA 1700020C11 gene	1700020C11Rik	-0.512	0.004
1452008_at	tetratricopeptide repeat domain 39B	Ttc39b	-0.512	0.000
1422624_at	REV1 homolog (S. cerevisiae)	Rev1	-0.511	0.003
1415767_at	YTH domain family 1	Ythdf1	-0.511	0.000
1425364_a_at	solute carrier family 3 (activators of dibasic and neutral amino acid transport), member 2	Slc3a2	-0.510	0.001
1452532_x_at	carcinoembryonic antigen-related cell adhesion molecule 1	Ceacam1	-0.510	0.001
1448978_at	neuronal guanine nucleotide exchange factor	Ngef	-0.509	0.003
1416662_at	sarcosine dehydrogenase	Sardh	-0.503	0.002
1429033_at	golgi coiled coil 1	Gcc1	-0.502	0.001
1460705_at	ribosomal protein S6 kinase, polypeptide 1	Rps6kb1	-0.502	0.001
1450068_at	bromodomain adjacent to zinc finger domain, 1B	Baz1b	-0.498	0.002
1437102_at	YTH domain family 1	Ythdf1	-0.494	0.001
1451554_a_at	anterior pharynx defective 1a homolog (C. elegans)	Aph1a	-0.494	0.001
1450869_at	fibroblast growth factor 1	Fgf1	-0.494	0.005
1450983_at	A kinase (PRKA) anchor protein 8	Akap8	-0.489	0.000
1439061_at	coiled-coil domain containing 84	Ccdc84	-0.489	0.001
1434216_a_at	nudix (nucleoside diphosphate linked moiety X)-type motif 19	Nudt19	-0.488	0.003
1424590_at	DEAD (Asp-Glu-Ala-Asp) box polypeptide 19b	Ddx19b	-0.487	0.000
1417831_at	structural maintenance of chromosomes 1A	Smc1a	-0.487	0.002
1424558_a_at	calcium-binding tyrosine-(Y)-phosphorylation regulated (fibrousheathin 2)	Cabyr	-0.485	0.003
1426965_at	RAS related protein 2a	Rap2a	-0.484	0.006
1418801_at	zinc finger with KRAB and SCAN domains 1	Zkscan1	-0.483	0.001
1448780_at	solute carrier family 12, member 2	Slc12a2	-0.483	0.000
1434393_at	ubiquitin specific peptidase 34	Usp34	-0.481	0.002
1429005_at	malignant fibrous histiocytoma amplified sequence 1	Mfhas1	-0.478	0.001
1427440_a_at	afamin	Afm	-0.476	0.000
1460228_at	upstream transcription factor 2	Usf2	-0.475	0.000
1451388_a_at	ATPase, class VI, type 11B	Atp11b	-0.474	0.000
1428113_at	transmembrane and tetratricopeptide repeat containing 4	Tmtc4	-0.469	0.001
1442554_s_at	kalirin, RhoGEF kinase	Kalrn	-0.469	0.003
1420947_at	alpha thalassemia/mental retardation syndrome X-linked homolog (human)	Atrx	-0.468	0.002
1452333_at	SWI/SNF related, matrix associated, actin dependent regulator of chromatin, subfamily a, member 2	Smarca2	-0.468	0.004
1416403_at	ATP-binding cassette, sub-family B (MDR/TAP), member 10	Abcb10	-0.465	0.001
1450083_at	CCR4-NOT transcription complex, subunit 4	Cnot4	-0.463	0.000
1427027_a_at	general transcription factor III A	Gtf3a	-0.463	0.001
1415988_at	high density lipoprotein (HDL) binding protein	Hdlbp	-0.463	0.004
1417629_at	proline dehydrogenase	Prodh	-0.461	0.003
1449585_at	interleukin 1 receptor accessory protein	Il1rap	-0.461	0.003
1436343_at	chromodomain helicase DNA binding protein 4	Chd4	-0.460	0.000
1416265_at	calpain 10	Capn10	-0.460	0.003
1417973_at	inter-alpha trypsin inhibitor, heavy chain 1	Itih1	-0.459	0.006
1428872_at	male-specific lethal 1 homolog (Drosophila)	Msl1	-0.459	0.000
1425205_at	DEAD (Asp-Glu-Ala-Asp) box polypeptide 19b	Ddx19b	-0.459	0.000
1425619_s_at	desmoglein 2	Dsg2	-0.458	0.002
1449118_at	dihydrolipoamide branched chain transacylase E2	Dbt	-0.457	0.001

1450387_s_at	adenylate kinase 4	Ak4	-0.456	0.002
1455601_at	hypothetical LOC100504714	LOC100504714	-0.455	0.005
1424412_at	opioid growth factor receptor-like 1	Ogfrl1	-0.454	0.001
1449813_at	zinc finger protein 30	Zfp30	-0.453	0.004
1418294_at	erythrocyte protein band 4.1-like 4b	Epb4.1l4b	-0.452	0.000
1418453_a_at	ATPase, Na+/K+ transporting, beta 1 polypeptide	Atp1b1	-0.450	0.001
1421664_a_at	serine/threonine/tyrosine interaction protein	Styx	-0.450	0.000
1424586_at	EH domain binding protein 1	Ehbp1	-0.446	0.002
1424687_at	HEAT repeat containing 6	Heatr6	-0.445	0.003
1454636_at	chromobox homolog 5 (Drosophila HP1a)	Cbx5	-0.445	0.000
1417622_at	solute carrier family 12, member 2	Slc12a2	-0.442	0.002
1451819_at	zinc finger, SWIM domain containing 6	Zswim6	-0.441	0.000
1433851_at	protein phosphatase 4, regulatory subunit 2	Ppp4r2	-0.441	0.000
1427982_s_at	synaptic nuclear envelope 2	Syne2	-0.440	0.000
1451391_at	RIKEN cDNA 2700050L05 gene	2700050L05Rik	-0.439	0.005
1416708_a_at	GRAM domain containing 1A	Gramd1a	-0.438	0.002
1438115_a_at	solute carrier family 9 (sodium/hydrogen exchanger), member 3 regulator 1	Slc9a3r1	-0.438	0.001
1423493_a_at	nuclear factor I/X	Nfix	-0.437	0.001
1452009_at	tetratricopeptide repeat domain 39B	Ttc39b	-0.435	0.000
1426545_at	trinucleotide repeat containing 6b	Tnrc6b	-0.431	0.001
1449623_at	thioredoxin reductase 3	Txnrd3	-0.430	0.006
1426326_at	zinc finger protein 91	Zfp91	-0.430	0.003
1425991_a_at	KN motif and ankyrin repeat domains 2	Kank2	-0.430	0.004
1448426_at	sarcosine dehydrogenase	Sardh	-0.430	0.003
1421504_at	trans-acting transcription factor 4	Sp4	-0.429	0.001
1449374_at	pipecolic acid oxidase	Pipox	-0.428	0.000
1456088_at	X-linked inhibitor of apoptosis	Xiap	-0.428	0.003
1417823_at	glycine C-acetyltransferase (2-amino-3-ketobutyrate-coenzyme A ligase)	Gcat	-0.428	0.003
1423546_at	zinc finger protein 207	Zfp207	-0.428	0.001
1438116_x_at	solute carrier family 9 (sodium/hydrogen exchanger), member 3 regulator 1	Slc9a3r1	-0.427	0.001
1450982_at	solute carrier family 9 (sodium/hydrogen exchanger), member 3 regulator 1	Slc9a3r1	-0.427	0.002
1427699_a_at	protein tyrosine phosphatase, non-receptor type 11	Ptpn11	-0.426	0.002
1416360_at	sorting nexin 18	Snx18	-0.426	0.001
1425000_s_at	RIKEN cDNA 5430407P10 gene	5430407P10Rik	-0.425	0.001
1435666_at	microtubule associated serine/threonine kinase 3	Mast3	-0.425	0.006
1460384_a_at	AT rich interactive domain 4B (RBP1-like)	Arid4b	-0.424	0.001
1426584_a_at	sorbitol dehydrogenase	Sord	-0.424	0.003
1435364_at	cysteine and histidine rich 1	Cyhr1	-0.423	0.004
1418495_at	zinc finger CCCH type containing 8	Zc3h8	-0.420	0.004
1425210_s_at	zinc finger protein 84	Zfp84	-0.420	0.005
1452497_a_at	nuclear factor of activated T-cells, cytoplasmic, calcineurin-dependent 3	Nfatc3	-0.417	0.001
1420985_at	ash1 (absent, small, or homeotic)-like (Drosophila)	Ash1l	-0.417	0.001
1449740_s_at	desmoglein 2	Dsg2	-0.417	0.001
1427730_a_at	zinc finger protein 148	Zfp148	-0.415	0.000
1456405_at	death inducer-obliterator 1	Dido1	-0.414	0.001
1425617_at	DEAH (Asp-Glu-Ala-His) box polypeptide 9	Dhx9	-0.414	0.005
1444952_a_at	nuclear casein kinase and cyclin-dependent kinase substrate 1	Nucks1	-0.413	0.006
1436034_at	centrosomal protein 68	Cep68	-0.413	0.002
1423668_at	zinc finger, DHHC domain containing 14	Zdhhc14	-0.412	0.005
1448965_at	INO80 homolog (S. cerevisiae)	Ino80	-0.410	0.000
1420628_at	---	---	-0.409	0.000
1436462_at	predicted gene 14326 /// predicted gene 14399	Gm14326 /// Gm14399	-0.407	0.001
1418170_a_at	zinc finger, CCHC domain containing 14	Zcchc14	-0.407	0.000
1448545_at	syndecan 2	Sdc2	-0.406	0.004
1451448_a_at	RIKEN cDNA 1110005A03 gene	1110005A03Rik	-0.405	0.003
1437237_x_at	zinc finger protein 110	Zfp110	-0.405	0.006
1451624_a_at	phosphatase, orphan 2	Phospho2	-0.404	0.000
1416832_at	solute carrier family 39 (metal ion transporter), member 8	Slc39a8	-0.404	0.001
1450868_at	heparan-alpha-glucosaminide N-acetyltransferase	Hgsnat	-0.404	0.000
1433669_at	A kinase (PRKA) anchor protein 8	Akap8	-0.403	0.002
1452581_at	regulation of nuclear pre-mRNA domain containing 1B	Rprd1b	-0.401	0.004
1416661_at	eukaryotic translation initiation factor 3, subunit A	Eif3a	-0.401	0.002
1451523_a_at	MIF4G domain containing	Mif4gd	-0.400	0.001
1418238_at	Isovaleryl coenzyme A dehydrogenase	Ivd	-0.400	0.004
1427163_at	ubiquitin protein ligase E3 component n-recognin 2	Ubr2	-0.400	0.000
1424288_at	methylphosphate capping enzyme	Mepce	-0.399	0.002
1455073_at	cytidine and dCMP deaminase domain containing 1	Cdadc1	-0.397	0.000
1420142_s_at	proliferation-associated 2G4	Pa2g4	-0.397	0.005
1429783_at	PDZ and LIM domain 5	Pdlim5	-0.397	0.002
1425577_at	zinc finger, MYM-type 5	Zmym5	-0.396	0.005
1425230_at	N-acetylglutamate synthase	Nags	-0.396	0.003
1449257_at	DNA segment, Chr 11, Wayne State University 99, expressed	D11Wsu99e	-0.395	0.000
1455446_x_at	acyl-Coenzyme A dehydrogenase, short/branched chain	Acadsb	-0.394	0.005
1426381_at	peroxisome proliferative activated receptor, gamma, coactivator-related 1	Pprc1	-0.393	0.002
1417448_at	RIKEN cDNA 1810008A18 gene	1810008A18Rik	-0.392	0.003
1417532_at	cytochrome P450, family 2, subfamily j, polypeptide 5	Cyp2j5	-0.391	0.003
1419178_at	CD3 antigen, gamma polypeptide	Cd3g	-0.390	0.005
1439476_at	desmoglein 2	Dsg2	-0.387	0.001
1422064_a_at	zinc finger and BTB domain containing 20	Zbtb20	-0.386	0.000
1417549_at	zinc finger protein 68	Zfp68	-0.386	0.006
1416402_at	ATP-binding cassette, sub-family B (MDR/TAP), member 10	Abcb10	-0.385	0.000
1437649_x_at	peptidylprolyl isomerase B	Ppib	-0.384	0.001
1451871_a_at	growth hormone receptor	Ghr	-0.384	0.002
1421478_a_at	zinc finger protein 318	Zfp318	-0.384	0.001
1448440_x_at	DNA segment, Chr 17, Wayne State University 104, expressed	D17Wsu104e	-0.383	0.003
1425085_at	RIKEN cDNA 6330416L07 gene	6330416L07Rik	-0.383	0.001
1418668_at	acyl-CoA synthetase medium-chain family member 1	Acsm1	-0.382	0.001
1460718_s_at	mitochondrial carrier homolog 1 (C. elegans)	Mtch1	-0.381	0.004
1426456_a_at	protein inhibitor of activated STAT 2	Pias2	-0.380	0.006

1425095_at	cDNA sequence BC002059	BC002059	-0.380	0.003
1451152_a_at	ATPase, Na+/K+ transporting, beta 1 polypeptide	Atp1b1	-0.380	0.006
1418432_at	calcium binding protein 39	Cab39	-0.379	0.004
1424657_at	TAO kinase 1	Taok1	-0.379	0.002
1455511_at	selenophosphate synthetase 1	Sephs1	-0.377	0.006
1451459_at	AT hook containing transcription factor 1	Ahctf1	-0.377	0.006
1425662_at	cytidine and dCMP deaminase domain containing 1	Cdadc1	-0.376	0.001
1429109_at	male-specific lethal 2 homolog (Drosophila)	Msl2	-0.376	0.004
1455955_s_at	sorting nexin 17	Snx17	-0.376	0.001
1422805_a_at	inhibitor of growth family, member 3	Ing3	-0.375	0.006
1416776_at	crystallin, mu	Crym	-0.375	0.001
1422769_at	synaptotagmin binding, cytoplasmic RNA interacting protein	Syncrip	-0.374	0.002
1451501_a_at	growth hormone receptor	Ghr	-0.374	0.000
1424926_at	SEC63-like (S. cerevisiae)	Sec63	-0.373	0.001
1452377_at	myeloid/lymphoid or mixed-lineage leukemia 1	Mll1	-0.372	0.001
1424810_at	taspase, threonine aspartase 1	Tasp1	-0.372	0.004
1434300_at	RIKEN cDNA 2610101N10 gene	2610101N10Rik	-0.372	0.001
1426546_at	testis-specific kinase 2	Tesk2	-0.372	0.000
1448905_at	mitochondrial ribosomal protein S34 /// non-metastatic cells 3, protein expressed in	Mrps34 /// Nme3	-0.371	0.001
1424860_at	RIKEN cDNA D930016D06 gene	D930016D06Rik	-0.371	0.001
1459900_at	expressed sequence C79468	C79468	-0.371	0.001
1438403_s_at	metastasis associated lung adenocarcinoma transcript 1 (non-coding RNA)	Malat1	-0.371	0.006
1436364_x_at	nuclear factor I/X	Nfix	-0.370	0.004
1418698_a_at	ferrochelatase	Fech	-0.369	0.000
1419508_at	receptor (TNFRSF)-interacting serine-threonine kinase 1	Ripk1	-0.369	0.001
1417309_at	transducer of ERBB2, 2	Tob2	-0.369	0.005
1422677_at	diacylglycerol O-acyltransferase 2	Dgat2	-0.369	0.004
1415730_at	cleavage and polyadenylation specific factor 7	Cpsf7	-0.368	0.003
1437236_a_at	zinc finger protein 110	Zfp110	-0.368	0.004
1426625_at	zinc finger protein 623	Zfp623	-0.366	0.002
1418397_at	zinc finger protein 275	Zfp275	-0.366	0.004
1434962_x_at	chemokine (C-C motif) ligand 27A /// chemokine (C-C motif) ligand 27b	Ccl27a /// Ccl27b	-0.366	0.002
1422787_at	FK506 binding protein-like	Fkbpl	-0.365	0.001
1451577_at	zinc finger and BTB domain containing 20	Zbtb20	-0.365	0.002
1420914_at	solute carrier organic anion transporter family, member 2a1	Slco2a1	-0.365	0.001
1421088_at	glypican 4	Gpc4	-0.364	0.001
1436833_x_at	tubulin tyrosine ligase-like 1	Ttll1	-0.363	0.002
1416800_at	transient receptor potential cation channel, subfamily M, member 7	Trpm7	-0.362	0.001
1423197_a_at	SMEK homolog 2, suppressor of mek1 (Dictyostelium)	Smek2	-0.361	0.002
1416681_at	ubiquitin protein ligase E3A	Ube3a	-0.360	0.006
1452396_at	serine/arginine-rich splicing factor 15	Srsf15	-0.359	0.002
1420917_at	PRP40 pre-mRNA processing factor 40 homolog A (yeast)	Prpf40a	-0.358	0.003
1453324_at	nuclear import 7 homolog (S. cerevisiae)	Nip7	-0.358	0.003
1423194_at	Rho GTPase activating protein 5	Arhgap5	-0.358	0.005
1449492_a_at	leukocyte cell-derived chemotaxin 2	Lect2	-0.357	0.001
1424883_s_at	serine/arginine-rich splicing factor 7	Srsf7	-0.357	0.005
1424244_at	RWD domain containing 4A	Rwdd4a	-0.357	0.006
1448851_a_at	DnaJ (Hsp40) homolog, subfamily C, member 5	Dnajc5	-0.357	0.003
1449069_at	zinc finger protein 148	Zfp148	-0.356	0.000
1455605_at	RUN and FYVE domain containing 3	Rufy3	-0.355	0.004
1437477_at	leucine rich repeat (in FLII) interacting protein 1	Lrrfip1	-0.354	0.003
1434177_at	endothelin converting enzyme 1	Ece1	-0.354	0.001
1455254_at	RIKEN cDNA 4833420G11 gene	4833420G11Rik	-0.354	0.001
1429186_a_at	cytidine and dCMP deaminase domain containing 1	Cdadc1	-0.353	0.003
1434311_at	CCR4-NOT transcription complex, subunit 6-like	Cnot6l	-0.353	0.003
1449382_at	solute carrier family 6 (neurotransmitter transporter, betaine/GABA), member 12	Slc6a12	-0.353	0.005
1423871_at	transmembrane protein 63a	Tmem63a	-0.352	0.004
1416042_s_at	nuclear autoantigenic sperm protein (histone-binding)	Nasp	-0.351	0.003
1448321_at	SPARC related modular calcium binding 1	Smoc1	-0.348	0.001
1416007_at	special AT-rich sequence binding protein 1	Satb1	-0.347	0.004
1424414_at	opioid growth factor receptor-like 1	Ogfrl1	-0.347	0.001
1418845_at	protein C	Proc	-0.346	0.000
1427456_at	WD repeat and FYVE domain containing 3	Wdfy3	-0.346	0.004
1421000_at	CCR4-NOT transcription complex, subunit 4	Cnot4	-0.345	0.002
1421127_at	transmembrane protein 42	Tmem42	-0.345	0.001
1460328_at	bromodomain containing 3	Brd3	-0.345	0.001
1452322_a_at	bromodomain and WD repeat domain containing 1	Brwd1	-0.345	0.005
1451019_at	cathepsin F	Ctsf	-0.345	0.005
1425956_a_at	cytidine and dCMP deaminase domain containing 1	Cdadc1	-0.344	0.002
1425279_at	PDLIM1 interacting kinase 1 like	Pdlk1l	-0.344	0.002
1448350_at	argininosuccinate lyase	Asl	-0.343	0.002
1452917_at	replication factor C (activator 1) 5	Rfc5	-0.343	0.005
1429052_at	protein tyrosine phosphatase, receptor type, D	Ptprd	-0.342	0.002
1423303_at	PAX interacting (with transcription-activation domain) protein 1	Paxip1	-0.340	0.001
1448229_s_at	cyclin D2	Ccnd2	-0.340	0.003
1452222_at	utrophin	Utrn	-0.339	0.003
1418023_at	N(alpha)-acetyltransferase 15, NatA auxiliary subunit	Naa15	-0.339	0.002
1452629_at	scaffold attachment factor B2	Safb2	-0.339	0.006
1437067_at	putative homeodomain transcription factor 2	Phtf2	-0.339	0.003
1448910_at	peroxisomal trans-2-enoyl-CoA reductase	Pecr	-0.338	0.001
1425157_x_at	tetraspanin 33	Tspan33	-0.338	0.004
1426798_a_at	protein phosphatase 1, regulatory (inhibitor) subunit 15b	Ppp1r15b	-0.338	0.002
1460681_at	carcinoembryonic antigen-related cell adhesion molecule 1	Ceacam1	-0.338	0.003
1423951_at	TM2 domain containing 3	Tm2d3	-0.337	0.001
1450942_at	zinc finger protein 830	Zfp830	-0.337	0.004
1424342_at	forty-two-three domain containing 1	Fyttd1	-0.337	0.001
1417261_at	mbt domain containing 1	Mbtd1	-0.337	0.005
1417538_at	solute carrier family 35 (CMP-sialic acid transporter), member 1	Slc35a1	-0.337	0.002
1424980_s_at	anterior pharynx defective 1a homolog (C. elegans)	Aph1a	-0.336	0.002

1426378_at	eukaryotic translation initiation factor 4B	Eif4b	-0.335	0.002
1422000_at	aldo-keto reductase family 1, member C12	Akr1c12	-0.334	0.003
1424120_at	ring finger protein 8	Rnf8	-0.334	0.001
1427776_a_at	fibroblast growth factor receptor 4	Fgfr4	-0.333	0.005
1424065_at	ER degradation enhancer, mannosidase alpha-like 1	Edem1	-0.333	0.001
1454641_at	CGG triplet repeat binding protein 1	Cggbp1	-0.333	0.001
1425200_at	chloride channel CLIC-like 1	Clcc1	-0.333	0.003
1456488_at	WD repeat domain 33	Wdr33	-0.333	0.001
1427408_a_at	thyroid hormone receptor associated protein 3	Thrap3	-0.331	0.003
1423869_s_at	thioredoxin reductase 3	Txnrd3	-0.331	0.003
1436158_at	eukaryotic translation initiation factor 4E binding protein 2	Eif4ebp2	-0.331	0.002
1426287_at	ataxin 7	Atxn7	-0.330	0.001
1436714_at	LIM domain containing preferred translocation partner in lipoma	Lpp	-0.330	0.002
1452200_at	CDKN2A interacting protein N-terminal like	Cdkn2aipnl	-0.330	0.001
1418366_at	histone cluster 2, H2aa1 /// histone cluster 2, H2aa2 /// histone cluster 2, H2ac /// histone cluster 2, H3c1	Hist2h2aa1 /// Hist2h2aa2 /// Hist2h2ac /// Hist2h3c1	-0.330	0.006
1418514_at	metal response element binding transcription factor 2	Mtf2	-0.330	0.004
1455026_at	sno, strawberry notch homolog 1 (Drosophila)	Sbno1	-0.330	0.003
1455625_at	TAF10 RNA polymerase II, TATA box binding protein (TBP)-associated factor	Taf10	-0.329	0.005
1455076_a_at	RIKEN cDNA 4933424B01 gene	4933424B01Rik	-0.329	0.001
1422678_at	diacylglycerol O-acyltransferase 2	Dgat2	-0.329	0.001
1417572_at	N-methylpurine-DNA glycosylase	Mpg	-0.328	0.005
1436167_at	Src homology 2 domain containing F	Shf	-0.327	0.001
1418577_at	tripartite motif-containing 8	Trim8	-0.326	0.002
1452099_at	expressed sequence AA408296	AA408296	-0.326	0.006
1460682_s_at	carcinoembryonic antigen-related cell adhesion molecule 1 /// carcinoembryonic antigen-related cell adhesion molecule 2	Ceacam1 /// Ceacam2	-0.326	0.005
1424485_at	angiopoietin-like 3	Angptl3	-0.325	0.002
1418190_at	paraoxonase 1	Pon1	-0.324	0.005
1436391_s_at	chloride channel CLIC-like 1	Clcc1	-0.324	0.001
1424166_at	mutS homolog 3 (E. coli)	Msh3	-0.323	0.006
1452126_at	zinc finger protein 160	Zfp160	-0.323	0.002
1416180_a_at	radixin	Rdx	-0.323	0.004
1433724_at	DNA segment, Chr 15, ERATO Doi 621, expressed	D15Ertd621e	-0.321	0.005
1457272_at	---	---	-0.321	0.006
1418445_at	solute carrier family 16 (monocarboxylic acid transporters), member 2	Slc16a2	-0.319	0.002
1428248_at	nuclear transcription factor, X-box binding 1	Nfx1	-0.319	0.004
1425319_s_at	small nuclear ribonucleoprotein 48 (U11/U12)	Snrnp48	-0.319	0.004
1437000_at	diacylglycerol kinase, theta	Dgkq	-0.318	0.002
1435742_at	SMEK homolog 1, suppressor of mek1 (Dictyostelium)	Smek1	-0.318	0.004
1424579_at	solute carrier family 35 (UDP-N-acetylglucosamine (UDP-GlcNAc) transporter), member 3	Slc35a3	-0.317	0.006
1437394_at	ArfGAP with GTPase domain, ankyrin repeat and PH domain 1	Agap1	-0.317	0.001
1426238_at	bone morphogenetic protein 1	Bmp1	-0.317	0.004
1452307_at	CDK5 and Abl enzyme substrate 2	Cables2	-0.317	0.004
1448767_s_at	gap junction protein, beta 1	Gjb1	-0.317	0.002
1427461_at	cDNA sequence BC005561	BC005561	-0.316	0.004
1427837_at	immunoglobulin kappa chain variable 32 (V32)	Igk-V32	-0.315	0.002
1423184_at	intersectin 2	Itsn2	-0.315	0.001
1449934_at	purine rich element binding protein A	Pura	-0.315	0.003
1449269_at	coagulation factor V	F5	-0.315	0.002
1427150_at	myeloid/lymphoid or mixed-lineage leukemia 3	Mll3	-0.315	0.004
1454899_at	LIM domain containing preferred translocation partner in lipoma	Lpp	-0.315	0.003
1432384_a_at	methyltransferase like 6	Mettl6	-0.315	0.003
1448439_at	DNA segment, Chr 17, Wayne State University 104, expressed	D17Wsu104e	-0.315	0.004
1417357_at	emerin	Emd	-0.315	0.004
1440195_at	serpine1 mRNA binding protein 1	Serbp1	-0.314	0.001
1417736_at	structural maintenance of chromosomes 6	Smc6	-0.314	0.001
1419867_a_at	ankyrin repeat and KH domain containing 1	Ankhd1	-0.314	0.003
1422619_at	phosphatidic acid phosphatase type 2A	Ppap2a	-0.314	0.005
1428029_a_at	H2A histone family, member V	H2afv	-0.313	0.002
1420641_a_at	sulfide quinone reductase-like (yeast)	Sqrdl	-0.312	0.003
1419172_at	dihydrofolate reductase	Dhfr	-0.312	0.001
1427384_at	chromodomain helicase DNA binding protein 6	Chd6	-0.312	0.003
1426380_at	eukaryotic translation initiation factor 4B	Eif4b	-0.312	0.002
1448670_at	ubiquitin-conjugating enzyme E2E 3, UBC4/5 homolog (yeast)	Ube2e3	-0.312	0.001
1429369_at	transportin 3	Tnpo3	-0.311	0.004
1437024_at	sphingomyelin phosphodiesterase 4	Smpd4	-0.311	0.005
1449042_at	CCCTC-binding factor	Ctcf	-0.311	0.002
1437511_x_at	chloride channel CLIC-like 1	Clcc1	-0.310	0.003
1448810_at	glucosamine	Gne	-0.309	0.006
1418900_at	ubiquitin-fold modifier 1	Ufm1	-0.309	0.004
1453080_at	male-specific lethal 2 homolog (Drosophila)	Msl2	-0.309	0.003
1460349_at	proline rich 14	Prr14	-0.308	0.004
1417084_at	eukaryotic translation initiation factor 4E binding protein 2	Eif4ebp2	-0.308	0.005
1452885_at	serine/arginine-rich splicing factor 2, interacting protein	Srsf2ip	-0.307	0.006
1424207_at	SWI/SNF related, matrix associated, actin dependent regulator of chromatin, subfamily a, member 5	Smarca5	-0.306	0.001
1424569_at	DEAD (Asp-Glu-Ala-Asp) box polypeptide 46	Ddx46	-0.305	0.005
1418699_s_at	ferrochelatase	Fech	-0.305	0.002
1421148_a_at	Tia1 cytotoxic granule-associated RNA binding protein-like 1	Tial1	-0.303	0.006
1454801_at	ankyrin repeat domain 28	Ankrd28	-0.302	0.002
1450050_at	histone cell cycle regulation defective homolog A (S. cerevisiae)	Hira	-0.302	0.003
1428092_at	cell division cycle 5-like (S. pombe)	Cdc5l	-0.302	0.003
1427232_at	teashirt zinc finger family member 1	Tshz1	-0.302	0.001
1423565_at	phosphoribosylaminoimidazole carboxylase, phosphoribosylaminoribosylaminoimidazole, succinocarboxamide synthetase	Paics	-0.301	0.003
1425793_a_at	RAR-related orphan receptor gamma	Rorc	-0.301	0.002
1449849_a_at	F-box and leucine-rich repeat protein 6	Fbxl6	-0.301	0.001
1450199_a_at	stabilin 1	Stab1	-0.301	0.005
1416913_at	carboxylesterase 1C	Ces1c	-0.300	0.005

1423396_at	angiotensinogen (serpin peptidase inhibitor, clade A, member 8)	Agt	-0.300	0.003
1419131_at	coagulation factor XIII, beta subunit	F13b	-0.299	0.006
1422665_a_at	protein-L-isoaspartate (D-aspartate) O-methyltransferase 1	Pcmt1	-0.299	0.004
1420372_at	syntrophin, basic 2	Sntb2	-0.299	0.006
1422453_at	pre-mRNA processing factor 8	Prpf8	-0.298	0.003
1418627_at	glutamate-cysteine ligase, modifier subunit	Gclm	-0.298	0.002
1448766_at	gap junction protein, beta 1	Gjb1	-0.297	0.006
1448026_at	chromodomain helicase DNA binding protein 7	Chd7	-0.296	0.004
1437382_at	activin receptor IIA	Acvr2a	-0.296	0.001
1416533_at	EGL nine homolog 2 (C. elegans)	Egln2	-0.296	0.003
1435524_at	small nucleolar RNA host gene 8	Snhg8	-0.295	0.005
1424316_at	solute carrier family 25 (mitochondrial thiamine pyrophosphate carrier), member 19	Slc25a19	-0.295	0.004
1419045_at	solute carrier family 25 (mitochondrial carrier; phosphate carrier), member 23	Slc25a23	-0.295	0.004
1449043_at	N-acetyl galactosaminidase, alpha	Naga	-0.295	0.004
1453993_a_at	BCL2/adenovirus E1B interacting protein 2	Bnip2	-0.295	0.002
1426243_at	cystathionase (cystathionine gamma-lyase)	Cth	-0.294	0.003
1417949_at	interleukin enhancer binding factor 2	Ilf2	-0.293	0.003
1452686_s_at	transmembrane protein 222	Tmem222	-0.293	0.001
1426775_s_at	secretory carrier membrane protein 1	Scamp1	-0.293	0.002
1426030_a_at	acylpeptide hydrolase	Apeh	-0.293	0.001
1449084_at	kallikrein B, plasma 1	Klkb1	-0.292	0.001
1426094_at	rhomboid, veinlet-like 1 (Drosophila)	Rhbdl1	-0.291	0.002
1415787_at	alpha glucosidase 2 alpha neutral subunit	Ganab	-0.291	0.005
1434612_s_at	sno, strawberry notch homolog 1 (Drosophila)	Sbno1	-0.291	0.003
1453124_at	transportin 3	Tnpo3	-0.290	0.005
1417834_at	synaptojanin 2 binding protein	Synj2bp	-0.289	0.001
1451221_at	cDNA sequence BC018507	BC018507	-0.288	0.004
1455066_s_at	melanoma inhibitory activity 3	Mia3	-0.288	0.004
1415920_at	cleavage stimulation factor, 3' pre-RNA subunit 2, tau	Cstf2t	-0.288	0.001
1449800_x_at	PHD finger protein 7	Phf7	-0.286	0.004
1416393_at	EMG1 nucleolar protein homolog (S. cerevisiae)	Emg1	-0.285	0.003
1418696_at	tetratricopeptide repeat domain 36	Ttc36	-0.285	0.001
1417548_at	squamous cell carcinoma antigen recognized by T-cells 3	Sart3	-0.284	0.003
1434892_x_at	retinoblastoma binding protein 4	Rbbp4	-0.283	0.005
1425190_a_at	phosphatase, orphan 2	Phospho2	-0.283	0.002
1452364_at	suppressor of zeste 12 homolog (Drosophila)	Suz12	-0.283	0.004
1416167_at	peroxiredoxin 4	Prdx4	-0.282	0.004
1437175_at	PDLIM1 interacting kinase 1 like	Pdik1l	-0.282	0.003
1450376_at	Max interacting protein 1	Mxi1	-0.282	0.005
1452499_a_at	kinesin family member 2A	Kif2a	-0.281	0.002
1426967_at	axin 1	Axin1	-0.280	0.004
1454802_x_at	ariadne homolog 2 (Drosophila)	Arih2	-0.280	0.004
1426487_a_at	retinoblastoma binding protein 6	Rbbp6	-0.280	0.003
1423060_at	proliferation-associated 2G4	Pa2g4	-0.280	0.004
1417371_at	pellino 1	Pell1	-0.279	0.004
1427136_s_at	serine/arginine-rich splicing factor 12	Srsf12	-0.279	0.005
1426483_at	protein-kinase, interferon-inducible double stranded RNA dependent inhibitor, repressor of (P58 repressor)	Prkrir	-0.278	0.002
1460244_at	ureidopropionase, beta	Upb1	-0.278	0.003
AFFX-BioB-M_at	---	---	-0.277	0.004
1419819_s_at	SEC63-like (S. cerevisiae)	Sec63	-0.276	0.002
1415716_a_at	predicted gene 9846 /// ribosomal protein S27	Gm9846 /// Rps27	-0.275	0.003
1418635_at	ets variant gene 3	Etv3	-0.274	0.002
1424924_at	SEC63-like (S. cerevisiae)	Sec63	-0.273	0.003
1416874_a_at	Paf1, RNA polymerase II associated factor, homolog (S. cerevisiae)	Paf1	-0.272	0.005
1434306_at	RAB3A interacting protein	Rab3ip	-0.272	0.003
1427333_s_at	serine/arginine-rich splicing factor 15	Srsf15	-0.272	0.003
1451565_s_at	urocanase domain containing 1	Uroc1	-0.272	0.004
1422517_a_at	zinc ribbon domain containing, 1	Znrd1	-0.271	0.006
1436300_at	dual serine/threonine and tyrosine protein kinase	Dstyk	-0.271	0.005
1427317_at	antigenic determinant of rec-A protein	Kin	-0.270	0.006
1454640_at	coiled-coil-helix-coiled-coil-helix domain containing 7	Chchd7	-0.269	0.006
1422680_at	Ctr9, Paf1/RNA polymerase II complex component, homolog (S. cerevisiae)	Ctr9	-0.269	0.006
1418706_at	solute carrier family 38, member 3	Slc38a3	-0.267	0.005
1423068_at	intraflagellar transport 172 homolog (Chlamydomonas)	Ift172	-0.267	0.003
1460358_s_at	nudix (nucleoside diphosphate linked moiety X)-type motif 22	Nudt22	-0.267	0.006
1425473_at	mediator complex subunit 17	Med17	-0.266	0.005
1436266_x_at	chromobox homolog 1 (Drosophila HP1 beta)	Cbx1	-0.265	0.002
1420339_at	mediator of cell motility 1	Memo1	-0.264	0.005
1426379_at	eukaryotic translation initiation factor 4B	Eif4b	-0.261	0.003
1457675_at	RIKEN cDNA 2510002D24 gene	2510002D24Rik	-0.260	0.005
1451348_at	DEP domain containing 6	Depdc6	-0.259	0.002
1452734_at	ribonuclease T2A /// ribonuclease T2B	Rnaset2a /// Rnaset2b	-0.259	0.006
1452628_at	BCL2-associated athanogene 5	Bag5	-0.256	0.005
1415712_at	zinc finger, RAN-binding domain containing 1	Zranb1	-0.255	0.002
1426245_s_at	microtubule-associated protein, RP/EB family, member 2	Mapre2	-0.254	0.005
1427209_at	bromodomain adjacent to zinc finger domain, 2A	Baz2a	-0.254	0.005
1460689_at	PPPDE peptidase domain containing 2	Pppde2	-0.253	0.006
1448288_at	nuclear factor I/B	Nfib	-0.252	0.002
1436291_a_at	dihydropyrimidinase	Dpys	-0.251	0.005
1448573_a_at	carcinoembryonic antigen-related cell adhesion molecule 10	Ceacam10	-0.251	0.004
1415764_at	zinc finger CCCH type containing 11A	Zc3h11a	-0.250	0.004
1423047_at	toll interacting protein	Tollip	-0.250	0.004
1452611_at	listerin E3 ubiquitin protein ligase 1	Ltn1	-0.250	0.006
1448567_at	transmembrane protein 115	Tmem115	-0.249	0.006
1425240_at	cDNA sequence BC011426	BC011426	-0.246	0.005
1426359_at	zinc finger CCCH type containing 11A	Zc3h11a	-0.244	0.003
1434317_s_at	testis expressed gene 10	Tex10	-0.242	0.005
1419402_at	meiosis-specific nuclear structural protein 1	Mns1	-0.242	0.005

1427978_at	RIKEN cDNA 4732418C07 gene	4732418C07Rik	-0.241	0.003
1449316_at	cytochrome P450, family 4, subfamily f, polypeptide 15	Cyp4f15	-0.240	0.006
1418022_at	N(alpha)-acetyltransferase 15, NatA auxiliary subunit	Naa15	-0.237	0.005
1416859_at	FK506 binding protein 3	Fkbp3	-0.237	0.005
1449040_a_at	selenophosphate synthetase 2	Sephs2	-0.236	0.005
1425621_at	tripartite motif-containing 35	Trim35	-0.236	0.006
1424086_at	OAF homolog (Drosophila)	Oaf	-0.235	0.005
1460691_at	zinc finger protein 598	Zfp598	-0.234	0.002
1455184_at	MOB1, Mps One Binder kinase activator-like 1A (yeast)	Mobkl1a	-0.232	0.006
1452299_at	WW domain containing E3 ubiquitin protein ligase 1	Wwp1	-0.231	0.005
1426388_s_at	receptor-like tyrosine kinase	Ryk	-0.231	0.004
1455129_at	metadherin	Mtdh	-0.228	0.006
1427896_at	suppressor of defective silencing 3 homolog (S. cerevisiae)	Suds3	-0.227	0.006
1416680_at	ubiquitin protein ligase E3A	Ube3a	-0.224	0.005
1416497_at	protein disulfide isomerase associated 4	Pdia4	-0.219	0.006
1452288_at	myotubularin related protein 10	Mtmr10	-0.207	0.005
1420021_s_at	suppressor of zeste 12 homolog (Drosophila)	Suz12	-0.202	0.005
1437670_x_at	CD151 antigen	Cd151	0.203	0.006
1453184_at	family with sequence similarity 83, member G	Fam83g	0.217	0.006
1448596_at	solute carrier family 6 (neurotransmitter transporter, creatine), member 8	Slc6a8	0.222	0.005
1434946_at	DnaJ (Hsp40) homolog, subfamily C, member 27	Dnajc27	0.228	0.005
1456085_x_at	CD151 antigen	Cd151	0.233	0.003
1460708_s_at	cell division cycle 42 homolog (S. cerevisiae)	Cdc42	0.236	0.005
1415842_at	MTOR associated protein, LST8 homolog (S. cerevisiae)	Mlst8	0.236	0.006
1421166_at	attractin	Atrn	0.237	0.004
1415724_a_at	cell division cycle 42 homolog (S. cerevisiae)	Cdc42	0.238	0.006
1426716_at	tudor domain containing 7	Tdrd7	0.239	0.005
1449574_a_at	cell division cycle 42 homolog (S. cerevisiae)	Cdc42	0.244	0.005
1417150_at	solute carrier family 6 (neurotransmitter transporter, serotonin), member 4	Slc6a4	0.244	0.005
1426128_a_at	potassium voltage-gated channel, subfamily Q, member 2	Kcnq2	0.246	0.006
1450708_at	secretogranin II	Scg2	0.246	0.005
1426400_a_at	calpain, small subunit 1	Capns1	0.251	0.003
1416009_at	tetraspanin 3	Tspan3	0.251	0.005
1421444_at	progesterone receptor	Pgr	0.254	0.006
1416266_at	prodynorphin	Pdyn	0.254	0.004
1460726_at	adenylosuccinate synthetase, non muscle	Adss	0.255	0.004
1425629_a_at	nucleolar protein family 6 (RNA-associated)	Nol6	0.255	0.004
1435323_a_at	membrane bound O-acyltransferase domain containing 1	Mboat1	0.258	0.002
1460307_at	thymoma viral proto-oncogene 3	Akt3	0.258	0.004
1451230_a_at	WW domain binding protein 5	Wbp5	0.260	0.005
1415918_a_at	triosephosphate isomerase 1	Tpi1	0.260	0.006
1449141_at	filamin binding LIM protein 1	Fblim1	0.260	0.004
1450671_at	crystallin, beta A1	Cryba1	0.261	0.005
1425665_a_at	signal recognition particle 54A /// signal recognition particle 54B /// signal recognition particle 54C	Srp54a /// Srp54b /// Srp54c	0.261	0.005
1426073_at	twisted gastrulation homolog 1 (Drosophila)	Twsg1	0.263	0.004
1450591_at	olfactory receptor 154	Olfr154	0.264	0.006
1425904_at	special AT-rich sequence binding protein 2	Satb2	0.264	0.002
1426067_x_at	chaperonin containing Tcp1, subunit 3 (gamma)	Cct3	0.265	0.002
1449549_at	ephrin B2	Efnb2	0.268	0.005
1437984_x_at	HLA-B-associated transcript 1A	Bat1a	0.271	0.005
1420817_at	tyrosine 3-monooxygenase/tryptophan 5-monooxygenase activation protein, gamma polypeptide	Ywhag	0.273	0.006
1428265_at	protein phosphatase 2 (formerly 2A), regulatory subunit A (PR 65), beta isoform	Ppp2r1b	0.273	0.003
1424718_at	microtubule-associated protein tau	Mapt	0.274	0.006
1439270_x_at	RAN, member RAS oncogene family	Ran	0.274	0.002
1424769_s_at	caldesmon 1	Cald1	0.276	0.003
1431726_a_at	transmembrane protein 80	Tmem80	0.276	0.004
1415941_s_at	zinc finger, AN1-type domain 2A	Zfand2a	0.280	0.002
1422507_at	cystatin B	Cstb	0.280	0.006
1454454_at	ELAV (embryonic lethal, abnormal vision, Drosophila)-like 2 (Hu antigen B)	Elavl2	0.280	0.006
1416596_at	solute carrier family 44, member 4	Slc44a4	0.280	0.002
1449222_at	Epstein-Barr virus induced gene 3	Ebi3	0.283	0.003
1422986_at	estrogen related receptor, beta	Esrrb	0.284	0.005
1427623_at	hect (homologous to the E6-AP (UBE3A) carboxyl terminus) domain and RCC1 (CHC1)-like domain (RLD) 2	Herc2	0.285	0.006
1422957_at	chemokine (C-C motif) receptor 3	Ccr3	0.285	0.004
1416156_at	vinculin	Vcl	0.287	0.004
1425217_a_at	synaptojanin 2	Synj2	0.288	0.006
1431692_a_at	Casitas B-lineage lymphoma c	Cblc	0.289	0.006
1448437_a_at	GTP binding protein 2	Gtpbp2	0.289	0.001
1418031_at	myosin IXb	Myo9b	0.290	0.005
1420943_at	zinc finger protein 185	Zfp185	0.290	0.006
1416905_at	guanylate cyclase activator 2a (guanylin)	Guca2a	0.290	0.002
1426672_at	anoctamin 10	Ano10	0.290	0.001
1456199_x_at	RAN binding protein 9	Ranbp9	0.291	0.001
1448736_a_at	hypoxanthine guanine phosphoribosyl transferase	Hprt	0.292	0.002
1424114_s_at	laminin B1	Lamb1	0.292	0.005
1418810_at	corticotropin releasing hormone receptor 1	Crhr1	0.293	0.002
1420376_a_at	H3 histone, family 3B	H3f3b	0.295	0.004
1448016_at	spindle assembly 6 homolog (C. elegans)	Sass6	0.295	0.004
1448210_at	RAB1, member RAS oncogene family	Rab1	0.297	0.003
1425676_a_at	elongation of very long chain fatty acids (FEN1/Elo2, SUR4/Elo3, yeast)-like 1	Elovl1	0.298	0.003
1450748_at	sphingomyelin phosphodiesterase 3, neutral	Smpd3	0.300	0.003
1418115_s_at	torsin A interacting protein 2	Tor1aip2	0.300	0.004
1427694_at	gonadotropin releasing hormone receptor	Gnrhr	0.303	0.006
1435110_at	unc-5 homolog B (C. elegans)	Unc5b	0.303	0.004
1449714_at	family with sequence similarity 73, member B	Fam73b	0.304	0.003
1449107_at	nudix (nucleoside diphosphate linked moiety X)-type motif 4	Nudt4	0.305	0.002
1420911_a_at	milk fat globule-EGF factor 8 protein	Mfge8	0.306	0.003
1434348_at	fasciculation and elongation protein zeta 2 (zygin II)	Fez2	0.308	0.004
1435659_a_at	triosephosphate isomerase 1	Tpi1	0.308	0.001

1450534_x_at	histocompatibility 2, K1, K region	H2-K1	0.310	0.004
1420820_at	RIKEN cDNA 2900073G15 gene	2900073G15Rik	0.311	0.003
1452246_at	osteoclast stimulating factor 1	Ostf1	0.318	0.006
1418164_at	syntaxin 2	Stx2	0.321	0.001
1423816_at	CAAX box 1 homolog A (human) /// CAAX box 1 homolog B (human)	Cxx1a /// Cxx1b	0.323	0.001
1460412_at	fibulin 7	Fbln7	0.323	0.001
1431697_at	synaptojanin 2	Synj2	0.325	0.002
1449885_at	transmembrane protein 47	Tmem47	0.326	0.004
1433558_at	disabled homolog 2 (Drosophila) interacting protein	Dab2ip	0.327	0.002
1425305_at	zinc finger protein 295	Zfp295	0.331	0.005
1451967_x_at	karyopherin (importin) beta 1	Kpnb1	0.335	0.003
1450191_a_at	SRY-box containing gene 13	Sox13	0.336	0.003
1438650_x_at	gap junction protein, alpha 1	Gja1	0.337	0.002
1427888_a_at	spectrin alpha 2	Spna2	0.337	0.004
1417432_a_at	guanine nucleotide binding protein (G protein), beta 1	Gnb1	0.338	0.001
1423228_at	UDP-Gal:betaGlcNAc beta 1,4-galactosyltransferase, polypeptide 6	B4galt6	0.338	0.006
1419182_at	sushi, von Willebrand factor type A, EGF and pentraxin domain containing 1	Svep1	0.338	0.002
1416897_at	poly (ADP-ribose) polymerase family, member 9	Parp9	0.340	0.005
1416001_a_at	coactosin-like 1 (Dictyostelium)	Cotl1	0.340	0.001
1417960_at	cytoplasmic polyadenylation element binding protein 1	Cpeb1	0.340	0.004
1421751_a_at	proteasome (prosome, macropain) 26S subunit, non-ATPase, 14	Psmd14	0.341	0.004
1424640_at	ADP-ribosylation factor-like 8A	Arl8a	0.342	0.004
1450010_at	hydroxysteroid (17-beta) dehydrogenase 12	Hsd17b12	0.343	0.004
1456193_x_at	glutathione peroxidase 4	Gpx4	0.344	0.005
1452152_at	clathrin interactor 1	Clint1	0.346	0.001
1419942_at	Sulfiredoxin 1 homolog (S. cerevisiae)	Srxn1	0.347	0.003
1438977_x_at	RAN, member RAS oncogene family	Ran	0.347	0.001
1449670_x_at	G protein-coupled receptor 137B	Gpr137b	0.349	0.005
1435979_a_at	myosin XVB	Myo15b	0.350	0.000
1421792_s_at	triggering receptor expressed on myeloid cells 2	Trem2	0.351	0.004
AFFX-GapdhMur/M32599_3_at	glyceraldehyde-3-phosphate dehydrogenase	Gapdh	0.352	0.006
1430029_a_at	tetraspanin 31	Tspan31	0.353	0.006
1428141_at	golgi associated, gamma adaptin ear containing, ARF binding protein 2	Gga2	0.358	0.005
1425156_at	guanylate binding protein 6	Gbp6	0.358	0.002
1435830_a_at	RIKEN cDNA 5430435G22 gene	5430435G22Rik	0.359	0.001
1449682_s_at	tubulin, beta 2a, pseudogene 2 /// tubulin, beta 2B	Tubb2a-ps2 /// Tubb2b	0.360	0.003
1428699_at	spermine synthase	Sms	0.361	0.001
1415968_a_at	kidney androgen regulated protein	Kap	0.362	0.001
1448534_at	signal-regulatory protein alpha	Sirpa	0.363	0.003
1423584_at	insulin-like growth factor binding protein 7	Igfbp7	0.364	0.005
1450666_s_at	ataxin 10	Atxn10	0.365	0.001
1426210_x_at	poly (ADP-ribose) polymerase family, member 3	Parp3	0.365	0.006
1450011_at	hydroxysteroid (17-beta) dehydrogenase 12	Hsd17b12	0.366	0.001
1433883_at	tropomyosin 4	Tpm4	0.366	0.001
1426540_at	endonuclease domain containing 1	Endod1	0.367	0.004
1449110_at	ras homolog gene family, member B	Rhob	0.370	0.003
1435270_x_at	N-6 adenine-specific DNA methyltransferase 2 (putative)	N6amt2	0.370	0.004
1417358_s_at	sorbin and SH3 domain containing 1	Sorbs1	0.371	0.001
1438958_x_at	FK506 binding protein 1a	Fkbp1a	0.377	0.000
1417435_at	like-glycosyltransferase	Large	0.378	0.003
1423630_at	cytoglobin	Cygb	0.379	0.002
1454086_a_at	LIM domain only 2	Lmo2	0.380	0.002
1417702_a_at	histamine N-methyltransferase	Hnmt	0.382	0.002
1416004_at	tyrosine 3-monooxygenase/tryptophan 5-monooxygenase activation protein, eta polypeptide	Ywhah	0.383	0.001
1448870_at	latent transforming growth factor beta binding protein 1	Ltbp1	0.383	0.003
1424784_at	predicted gene 13139	Gm13139	0.383	0.003
1460318_at	cysteine and glycine-rich protein 3	Csrp3	0.385	0.005
1449041_a_at	thyroid hormone receptor interactor 6	Trip6	0.385	0.004
1416230_at	riboflavin kinase	Rfk	0.389	0.000
1434578_x_at	RAN, member RAS oncogene family	Ran	0.390	0.001
1427951_s_at	coiled-coil domain containing 28A	Ccdc28a	0.391	0.004
1418616_at	v-maf musculoaponeurotic fibrosarcoma oncogene family, protein K (avian)	Mafk	0.392	0.001
1436677_at	RIKEN cDNA 1810032O08 gene	1810032O08Rik	0.393	0.004
1449430_a_at	trehalase (brush-border membrane glycoprotein)	Treh	0.393	0.005
1420915_at	signal transducer and activator of transcription 1	Stat1	0.394	0.003
1416315_at	abhydrolase domain containing 4	Abhd4	0.395	0.000
1450642_at	SECIS binding protein 2-like	Secisbp2l	0.397	0.002
1439255_s_at	G protein-coupled receptor 137B /// G protein-coupled receptor 137B, pseudogene	Gpr137b /// Gpr137b-ps	0.397	0.002
1421217_a_at	lectin, galactose binding, soluble 9	Lgals9	0.399	0.006
1450012_x_at	tyrosine 3-monooxygenase/tryptophan 5-monooxygenase activation protein, gamma polypeptide	Ywhag	0.400	0.004
1460262_a_at	RIKEN cDNA 1700037H04 gene	1700037H04Rik	0.400	0.002
1416556_at	tetraspanin 31	Tspan31	0.402	0.002
1437172_x_at	hydroxyacyl-Coenzyme A dehydrogenase/3-ketoacyl-Coenzyme A thiolase /enoyl-Coenzyme A hydratase (trifunctional protein), beta subunit	Hadhb	0.403	0.003
1418848_at	aquaporin 7	Aqp7	0.405	0.006
1439367_x_at	ADP-ribosylation factor 4	Arf4	0.405	0.004
1450034_at	signal transducer and activator of transcription 1	Stat1	0.405	0.001
1448770_a_at	ATPase inhibitory factor 1	Atpif1	0.405	0.002
1422506_a_at	cystatin B	Cstb	0.407	0.000
1450033_a_at	signal transducer and activator of transcription 1	Stat1	0.407	0.001
1452344_at	synaptojanin 2	Synj2	0.409	0.002
1435680_a_at	dipeptidylpeptidase 7	Dpp7	0.410	0.001
1451511_at	3-hydroxyisobutyryl-Coenzyme A hydrolase	Hibch	0.411	0.005
1451695_a_at	glutathione peroxidase 4	Gpx4	0.412	0.003
1449368_at	decorin	Dcn	0.413	0.002
1451413_at	calpastatin	Cast	0.413	0.000
1419721_at	niacin receptor 1	Niacr1	0.414	0.003
1428465_at	transmembrane protein 147	Tmem147	0.416	0.001
1416304_at	LPS-induced TN factor	Litaf	0.417	0.005

1436479_a_at	dipeptidylpeptidase 7	Dpp7	0.417	0.000
1424155_at	fatty acid binding protein 4, adipocyte	Fabp4	0.419	0.002
1423986_a_at	shisa homolog 5 (Xenopus laevis)	Shisa5	0.419	0.004
1417251_at	palmdelphin	Palmd	0.419	0.005
1437992_x_at	gap junction protein, alpha 1	Gja1	0.420	0.004
1416658_at	frizzled-related protein	Frzb	0.422	0.005
1451224_at	secretory carrier membrane protein 5	Scamp5	0.424	0.004
1420997_a_at	glucose phosphate isomerase 1	Gpi1	0.424	0.004
1417355_at	paternally expressed 3	Peg3	0.426	0.003
1417384_at	ectonucleoside triphosphate diphosphohydrolase 5	Entpd5	0.429	0.006
1416808_at	nidogen 1	Nid1	0.429	0.001
1450985_a_at	tight junction protein 2	Tjp2	0.431	0.002
1419401_at	ankyrin repeat and SOCS box-containing 13	Asb13	0.431	0.003
1456196_x_at	FK506 binding protein 1a	Fkbp1a	0.435	0.001
1455581_x_at	hypothetical protein 9530028C05	9530028C05	0.436	0.004
1453939_x_at	predicted gene 9706	Gm9706	0.436	0.005
1432827_x_at	ubiquitin C	Ubc	0.437	0.004
1418714_at	dual specificity phosphatase 8	Dusp8	0.438	0.006
1424246_a_at	testis derived transcript	Tes	0.438	0.005
1422662_at	lectin, galactose binding, soluble 8	Lgals8	0.439	0.000
1448961_at	phospholipid scramblase 2	Plscr2	0.442	0.006
1450081_x_at	glucose phosphate isomerase 1	Gpi1	0.444	0.001
1429775_a_at	G protein-coupled receptor 137B /// G protein-coupled receptor 137B, pseudogene	Gpr137b /// Gpr137b-ps	0.445	0.002
1415911_at	imprinted and ancient	Impact	0.447	0.006
1426004_a_at	transglutaminase 2, C polypeptide	Tgm2	0.447	0.001
1425405_a_at	adenosine deaminase, RNA-specific	Adar	0.449	0.003
AFFX-GapdhMur/M32599_M_at	glyceraldehyde-3-phosphate dehydrogenase	Gapdh	0.449	0.003
1448184_at	FK506 binding protein 1a	Fkbp1a	0.451	0.000
1438360_x_at	solute carrier family 25 (mitochondrial carrier, adenine nucleotide translocator), member 5	Slc25a5	0.454	0.002
1427683_at	early growth response 2	Egr2	0.455	0.001
1427685_a_at	synaptojanin 2	Synj2	0.456	0.003
1426064_at	cytochrome P450, family 3, subfamily a, polypeptide 44	Cyp3a44	0.457	0.002
1433702_at	endoplasmic reticulum metallopeptidase 1	Ermp1	0.457	0.004
1424138_at	rhomboid family 1 (Drosophila)	Rhbdf1	0.457	0.001
1416229_at	riboflavin kinase	Rfk	0.458	0.000
1426098_a_at	calpastatin	Cast	0.460	0.000
1450429_at	calpain 6	Capn6	0.460	0.001
1421685_at	C-type lectin domain family 4, member b1	Clec4b1	0.464	0.002
1427079_at	microtubule-associated protein, RP/EB family, member 3	Mapre3	0.464	0.000
1416036_at	FK506 binding protein 1a	Fkbp1a	0.467	0.000
AFFX-GapdhMur/M32599_5_at	glyceraldehyde-3-phosphate dehydrogenase	Gapdh	0.467	0.001
1450918_s_at	Rous sarcoma oncogene	Src	0.468	0.001
1418386_at	N-6 adenine-specific DNA methyltransferase 2 (putative)	N6amt2	0.469	0.001
1437666_x_at	ubiquitin C	Ubc	0.471	0.005
1415800_at	gap junction protein, alpha 1	Gja1	0.471	0.006
1428803_at	acyl-CoA thioesterase 6	Acot6	0.473	0.006
1449072_a_at	N-6 adenine-specific DNA methyltransferase 2 (putative)	N6amt2	0.474	0.000
1451421_a_at	rogdi homolog (Drosophila)	Rogdi	0.475	0.003
1422161_at	sialic acid binding Ig-like lectin 1, sialoadhesin	Siglec1	0.479	0.000
1435454_a_at	cDNA sequence BC006779	BC006779	0.480	0.005
1419704_at	cytochrome P450, family 3, subfamily a, polypeptide 41A /// cytochrome P450, family 3, subfamily a, polypeptide 41B	Cyp3a41a /// Cyp3a41b	0.481	0.001
1423269_a_at	neural precursor cell expressed, developmentally down-regulated gene 4-like	Nedd4l	0.481	0.002
1434814_x_at	glucose phosphate isomerase 1	Gpi1	0.483	0.000
1448491_at	enoyl coenzyme A hydratase 1, peroxisomal	Ech1	0.484	0.000
1426376_at	receptor accessory protein 5	Reep5	0.486	0.001
1436320_at	---	---	0.488	0.004
1451036_at	spastic paraplegia 21 homolog (human)	Spg21	0.488	0.001
1434380_at	guanylate binding protein 6	Gbp6	0.488	0.002
1426434_at	transmembrane protein 43	Tmem43	0.489	0.001
1418500_at	nucleosome assembly protein 1-like 3	Nap1l3	0.491	0.002
1426529_a_at	transgelin 2	Tagln2	0.492	0.000
1422661_at	lectin, galactose binding, soluble 8	Lgals8	0.492	0.000
1425826_a_at	sorbin and SH3 domain containing 1	Sorbs1	0.492	0.005
1416101_a_at	histone cluster 1, H1c	Hist1h1c	0.497	0.000
1427345_a_at	sulfotransferase family 1A, phenol-preferring, member 1	Sult1a1	0.501	0.002
1456733_x_at	serine (or cysteine) peptidase inhibitor, clade H, member 1	Serpinh1	0.502	0.000
1426785_s_at	monoglyceride lipase	Mgll	0.505	0.006
1418572_x_at	tumor necrosis factor receptor superfamily, member 12a	Tnfrsf12a	0.506	0.005
1417879_at	neuron derived neurotrophic factor	Nenf	0.507	0.005
1418595_at	perilipin 4	Plin4	0.509	0.001
1425065_at	2'-5' oligoadenylate synthetase 2	Oas2	0.510	0.000
1417112_at	ADP-ribosylation factor-like 2 binding protein	Arl2bp	0.510	0.003
1439451_x_at	G protein-coupled receptor 172B	Gpr172b	0.512	0.001
1452227_at	sel-1 suppressor of lin-12-like 3 (C. elegans)	Sel1l3	0.522	0.001
1439259_x_at	abhydrolase domain containing 4	Abhd4	0.525	0.000
1419518_at	tubulin, alpha 8	Tuba8	0.526	0.002
1434553_at	transmembrane protein 56	Tmem56	0.527	0.000
1422609_at	cAMP-regulated phosphoprotein 19	Arpp19	0.527	0.004
1426541_a_at	endonuclease domain containing 1	Endod1	0.528	0.006
1450767_at	neural precursor cell expressed, developmentally down-regulated gene 9	Nedd9	0.528	0.001
1448605_at	ras homolog gene family, member C	Rhoc	0.528	0.004
1448211_at	ATPase, H+ transporting, lysosomal V0 subunit E2	Atp6v0e2	0.530	0.000
1418711_at	platelet derived growth factor, alpha	Pdgfa	0.532	0.002
1416868_at	cyclin-dependent kinase inhibitor 2C (p18, inhibits CDK4)	Cdkn2c	0.532	0.002
1434866_x_at	carnitine palmitoyltransferase 1a, liver	Cpt1a	0.537	0.003
1450355_a_at	capping protein (actin filament), gelsolin-like	Capg	0.537	0.006
1422403_at	predicted gene 12597 /// predicted gene 13280 /// interferon alpha 1 /// interferon alpha 12 /// interferon alpha 5 /// interferon alpha 6	Gm12597 /// Gm13280 /// Ifna1 /// Ifna12 /// Ifna5 /// Ifna6 /// Ifna7 /// Ifna9 /// Ifnab	0.541	0.000

	/// interferon alpha 7 /// interferon alpha 9 /// interferon alpha B			
1417703_at	poliovirus receptor-related 2	Pvrl2	0.542	0.006
1422576_at	ataxin 10	Atxn10	0.545	0.000
1456542_s_at	glutaminyl-tRNA synthase (glutamine-hydrolyzing)-like 1	Qrsl1	0.548	0.000
1427895_at	RIKEN cDNA 2310004N24 gene	2310004N24Rik	0.550	0.003
1427489_at	integrin alpha 8	Itga8	0.561	0.004
1424399_at	uridine-cytidine kinase 1	Uck1	0.563	0.001
1418825_at	immunity-related GTPase family M member 1	Irgm1	0.564	0.003
1416645_a_at	alpha fetoprotein	Afp	0.564	0.003
1460674_at	progestin and adipoQ receptor family member VII	Paqr7	0.566	0.001
1453836_a_at	monoglyceride lipase	Mgll	0.567	0.006
1436737_a_at	sorbin and SH3 domain containing 1	Sorbs1	0.567	0.000
1455908_a_at	serine carboxypeptidase 1	Scpep1	0.568	0.002
1418069_at	apolipoprotein C-II	Apoc2	0.568	0.003
1455900_x_at	transglutaminase 2, C polypeptide	Tgm2	0.569	0.003
1418260_at	hormonally upregulated Neu-associated kinase	Hunk	0.570	0.000
1425351_at	sulfiredoxin 1 homolog (S. cerevisiae)	Srxn1	0.571	0.001
1456466_x_at	ataxin 10	Atxn10	0.573	0.000
1416444_at	elongation of very long chain fatty acids (FEN1/Elo2, SUR4/Elo3, yeast)-like 2	Elovl2	0.576	0.002
1420979_at	p21 protein (Cdc42/Rac)-activated kinase 1	Pak1	0.576	0.006
1418911_s_at	acyl-CoA synthetase long-chain family member 4	Acsl4	0.578	0.000
1422701_at	zeta-chain (TCR) associated protein kinase	Zap70	0.579	0.001
1418449_at	ladinin	Lad1	0.580	0.001
1415779_s_at	actin, gamma, cytoplasmic 1	Actg1	0.584	0.006
1426774_at	poly (ADP-ribose) polymerase family, member 12	Parp12	0.586	0.001
1420726_x_at	trimethyllysine hydroxylase, epsilon	Tmlhe	0.588	0.001
1424373_at	armadillo repeat containing, X-linked 3	Armcx3	0.589	0.001
1424354_at	transmembrane protein 140	Tmem140	0.592	0.004
1434436_at	microrchidia 4	Morc4	0.593	0.005
1437465_a_at	prolyl 4-hydroxylase, beta polypeptide	P4hb	0.593	0.000
1436994_a_at	histone cluster 1, H1c	Hist1h1c	0.594	0.003
1426348_at	collagen, type IV, alpha 1	Col4a1	0.596	0.001
1438653_x_at	ataxin 10	Atxn10	0.605	0.000
1416454_s_at	actin, alpha 2, smooth muscle, aorta	Acta2	0.606	0.004
1421031_a_at	RIKEN cDNA 2310016C08 gene	2310016C08Rik	0.610	0.004
1417116_at	solute carrier family 6 (neurotransmitter transporter, creatine), member 8	Slc6a8	0.611	0.000
1449818_at	ATP-binding cassette, sub-family B (MDR/TAP), member 4	Abcb4	0.612	0.000
1418686_at	2'-5' oligoadenylate synthetase 1C	Oas1c	0.615	0.000
1426894_s_at	family with sequence similarity 102, member A	Fam102a	0.617	0.004
1420727_a_at	trimethyllysine hydroxylase, epsilon	Tmlhe	0.619	0.000
1421622_a_at	Rap guanine nucleotide exchange factor (GEF) 4	Rapgef4	0.620	0.003
1417965_at	pleckstrin homology domain containing, family A (phosphoinositide binding specific) member 1	Plekha1	0.622	0.000
1448169_at	keratin 18	Krt18	0.630	0.000
1426276_at	interferon induced with helicase C domain 1	Ifih1	0.631	0.002
1417434_at	glycerol phosphate dehydrogenase 2, mitochondrial	Gpd2	0.633	0.002
1451336_at	lectin, galactose binding, soluble 4	Lgals4	0.635	0.002
1435525_at	potassium channel tetramerisation domain containing 17	Kctd17	0.636	0.001
1427878_at	RIKEN cDNA 0610010O12 gene	0610010O12Rik	0.638	0.000
1423680_at	fatty acid desaturase 1	Fads1	0.638	0.004
1443969_at	insulin receptor substrate 2	Irs2	0.644	0.002
1434628_a_at	rhophilin, Rho GTPase binding protein 2	Rhpn2	0.651	0.001
1456494_a_at	tripartite motif-containing 30A /// tripartite motif-containing 30D	Trim30a /// Trim30d	0.656	0.006
1425913_a_at	spermatogenesis associated, serine-rich 2-like	Spats2l	0.660	0.004
1448380_at	lectin, galactoside-binding, soluble, 3 binding protein	Lgals3bp	0.661	0.000
1421362_a_at	fyn-related kinase	Frk	0.662	0.001
1426906_at	myeloid nuclear differentiation antigen like	Mndal	0.663	0.003
1419398_a_at	receptor accessory protein 5	Reep5	0.672	0.001
1451828_a_at	acyl-CoA synthetase long-chain family member 4	Acsl4	0.673	0.004
1460690_at	family with sequence similarity 195, member B	Fam195b	0.674	0.000
1420725_at	trimethyllysine hydroxylase, epsilon	Tmlhe	0.676	0.000
1435394_s_at	ras homolog gene family, member C	Rhoc	0.677	0.001
1424962_at	transmembrane 4 superfamily member 4	Tm4sf4	0.681	0.000
1438001_x_at	receptor accessory protein 5	Reep5	0.684	0.000
1422824_s_at	epidermal growth factor receptor pathway substrate 8	Eps8	0.694	0.005
1421679_a_at	cyclin-dependent kinase inhibitor 1A (P21)	Cdkn1a	0.694	0.005
1428066_at	coiled-coil domain containing 120	Ccdc120	0.695	0.000
1450127_a_at	glucagon receptor	Gcgr	0.695	0.000
1450696_at	proteasome (prosome, macropain) subunit, beta type 9 (large multifunctional peptidase 2)	Psmb9	0.700	0.000
1421998_at	torsin family 3, member A	Tor3a	0.705	0.006
1424921_at	bone marrow stromal cell antigen 2	Bst2	0.711	0.001
1428635_at	catechol-O-methyltransferase domain containing 1	Comtd1	0.716	0.003
1433531_at	acyl-CoA synthetase long-chain family member 4	Acsl4	0.722	0.000
1416591_at	RAB34, member of RAS oncogene family	Rab34	0.723	0.000
1427838_at	tubulin, beta 2A	Tubb2a	0.730	0.002
1423607_at	lumican	Lum	0.734	0.001
1435989_x_at	keratin 8	Krt8	0.734	0.000
1449442_at	peroxisomal biogenesis factor 11 alpha	Pex11a	0.734	0.005
1438169_a_at	FERM domain containing 4B	Frmd4b	0.737	0.004
1429947_a_at	Z-DNA binding protein 1	Zbp1	0.740	0.002
1448318_at	perilipin 2	Plin2	0.757	0.001
1419658_at	RIKEN cDNA C920025E04 gene	C920025E04Rik	0.763	0.002
1424528_at	cell growth regulator with EF hand domain 1	Cgref1	0.769	0.000
1424638_at	cyclin-dependent kinase inhibitor 1A (P21)	Cdkn1a	0.770	0.005
1450843_a_at	serine (or cysteine) peptidase inhibitor, clade H, member 1	Serpinh1	0.777	0.001
1448111_at	cytidine 5'-triphosphate synthase 2	Ctps2	0.785	0.006
1436172_at	hypothetical protein 9530028C05	9530028C05	0.790	0.002
1451860_a_at	tripartite motif-containing 30A	Trim30a	0.792	0.004
1431805_a_at	rhophilin, Rho GTPase binding protein 2	Rhpn2	0.794	0.000
1455918_at	adrenergic receptor, beta 3	Adrb3	0.796	0.006

1451680_at	sulfiredoxin 1 homolog (S. cerevisiae)	Srxn1	0.804	0.001
1417961_a_at	tripartite motif-containing 30A	Trim30a	0.805	0.005
1429159_at	inter-alpha (globulin) inhibitor H5	Itih5	0.807	0.002
1417757_at	unc-13 homolog B (C. elegans)	Unc13b	0.813	0.000
1425948_a_at	solute carrier family 25, member 30	Slc25a30	0.815	0.003
1420647_a_at	keratin 8	Krt8	0.815	0.000
1418280_at	Kruppel-like factor 6	Klf6	0.817	0.004
1423691_x_at	keratin 8	Krt8	0.819	0.000
1417860_a_at	spondin 2, extracellular matrix protein	Spon2	0.826	0.002
1449363_at	activating transcription factor 3	Atf3	0.834	0.001
1426989_at	calsyntenin 3	Clstn3	0.835	0.000
1424072_at	RIKEN cDNA 2010107G23 gene	2010107G23Rik	0.841	0.001
1451168_a_at	Rho GDP dissociation inhibitor (GDI) alpha	Arhgdia	0.847	0.000
1454078_a_at	galactose-3-O-sulfotransferase 1	Gal3st1	0.848	0.002
1449025_at	interferon-induced protein with tetratricopeptide repeats 3	Ifit3	0.849	0.005
1431591_s_at	predicted gene 9706 /// ISG15 ubiquitin-like modifier	Gm9706 /// Isg15	0.853	0.003
1450061_at	ectodermal-neural cortex 1	Enc1	0.869	0.001
1438676_at	macrophage activation 2 like	Mpa2l	0.878	0.001
1416431_at	tubulin, beta 6	Tubb6	0.881	0.000
1417982_at	insulin induced gene 2	Insig2	0.889	0.002
1453128_at	lymphatic vessel endothelial hyaluronan receptor 1	Lyve1	0.905	0.000
1451777_at	DEAD (Asp-Glu-Ala-Asp) box polypeptide 60	Ddx60	0.918	0.001
1418392_a_at	guanylate binding protein 3	Gbp3	0.928	0.000
1453196_a_at	2'-5' oligoadenylate synthetase-like 2	Oasl2	0.928	0.004
1417266_at	chemokine (C-C motif) ligand 6	Ccl6	0.936	0.006
1451488_at	fat storage-inducing transmembrane protein 1	Fitm1	0.938	0.000
1423933_a_at	RIKEN cDNA 1600029D21 gene	1600029D21Rik	0.952	0.000
1426875_s_at	sulfiredoxin 1 homolog (S. cerevisiae)	Srxn1	0.952	0.001
1449984_at	chemokine (C-X-C motif) ligand 2	Cxcl2	0.956	0.001
1433508_at	Kruppel-like factor 6	Klf6	0.963	0.001
1417981_at	insulin induced gene 2	Insig2	0.965	0.001
1453181_x_at	phospholipid scramblase 1	Plscr1	0.986	0.000
1424518_at	apolipoprotein L 9a /// apolipoprotein L 9b	Apol9a /// Apol9b	0.990	0.002
1424007_at	growth differentiation factor 10	Gdf10	0.995	0.005
1427002_s_at	arylsulfatase G	Arsg	1.001	0.000
1424140_at	galactose-4-epimerase, UDP	Gale	1.004	0.002
1449968_s_at	acyl-CoA thioesterase 10 /// acyl-CoA thioesterase 9	Acot10 /// Acot9	1.009	0.001
1418073_at	acyl-CoA thioesterase 9	Acot9	1.009	0.001
1451426_at	DEXH (Asp-Glu-X-His) box polypeptide 58	Dhx58	1.015	0.000
1450352_at	melatonin receptor 1A	Mtnr1a	1.017	0.000
1436186_at	E2F transcription factor 8	E2f8	1.021	0.000
1448272_at	B-cell translocation gene 2, anti-proliferative	Btg2	1.021	0.000
1427742_a_at	Kruppel-like factor 6	Klf6	1.028	0.002
1425964_x_at	heat shock protein 1	Hspb1	1.040	0.000
1451780_at	B-cell linker	Blnk	1.063	0.002
1422943_a_at	heat shock protein 1	Hspb1	1.068	0.000
1416250_at	B-cell translocation gene 2, anti-proliferative	Btg2	1.075	0.000
1452661_at	transferrin receptor	Tfrc	1.085	0.000
1418293_at	interferon-induced protein with tetratricopeptide repeats 2	Ifit2	1.087	0.000
1417980_a_at	insulin induced gene 2	Insig2	1.098	0.000
1416021_a_at	fatty acid binding protein 5, epidermal /// predicted gene 3601	Fabp5 /// Gm3601	1.099	0.002
1425567_a_at	annexin A5	Anxa5	1.107	0.000
1449757_x_at	deoxynucleotidyltransferase, terminal	Dntt	1.118	0.001
1460351_at	S100 calcium binding protein A11 (calgizzarin)	S100a11	1.121	0.003
1456642_x_at	S100 calcium binding protein A10 (calpactin)	S100a10	1.140	0.001
1429527_a_at	phospholipid scramblase 1	Plscr1	1.150	0.000
1420715_a_at	peroxisome proliferator activated receptor gamma	Pparg	1.156	0.006
1419031_at	fatty acid desaturase 2	Fads2	1.159	0.000
1416762_at	S100 calcium binding protein A10 (calpactin)	S100a10	1.163	0.001
1418123_at	unc-119 homolog (C. elegans)	Unc119	1.168	0.002
1418580_at	receptor transporter protein 4	Rtp4	1.177	0.000
1436890_at	UDP-N-acteylglucosamine pyrophosphorylase 1-like 1	Uap1l1	1.177	0.000
1436504_x_at	apolipoprotein A-IV	Apoa4	1.180	0.000
1452277_at	arylsulfatase G	Arsg	1.181	0.000
1424339_at	2'-5' oligoadenylate synthetase-like 1	Oasl1	1.184	0.001
1422804_at	serine (or cysteine) peptidase inhibitor, clade B, member 6b	Serpinb6b	1.187	0.002
1450484_a_at	cytidine monophosphate (UMP-CMP) kinase 2, mitochondrial	Cmpk2	1.202	0.002
1427912_at	carbonyl reductase 3	Cbr3	1.210	0.000
1429379_at	lymphatic vessel endothelial hyaluronan receptor 1	Lyve1	1.213	0.000
1425120_x_at	interferon, alpha-inducible protein 27 like 2B	Ifi27l2b	1.219	0.000
1416022_at	fatty acid binding protein 5, epidermal	Fabp5	1.260	0.003
1417389_at	glypican 1	Gpc1	1.261	0.001
1417244_a_at	interferon regulatory factor 7	Irf7	1.263	0.000
1419091_a_at	annexin A2	Anxa2	1.263	0.001
1420603_s_at	retinoic acid early transcript 1, alpha /// retinoic acid early transcript beta /// retinoic acid early transcript gamma /// retinoic acid early transcript delta /// retinoic acid early transcript 1E	Raet1a /// Raet1b /// Raet1c /// Raet1d /// Raet1e	1.271	0.000
1450545_a_at	deoxynucleotidyltransferase, terminal	Dntt	1.274	0.002
1448694_at	Jun oncogene	Jun	1.298	0.000
1435792_at	component of Sp100-rs /// predicted gene 7592	Csprs /// Gm7592	1.332	0.000
1449325_at	fatty acid desaturase 2	Fads2	1.339	0.000
1420835_at	solute carrier family 25, member 30	Slc25a30	1.419	0.000
1424626_at	RIKEN cDNA 2010003K11 gene	2010003K11Rik	1.431	0.001
1417761_at	apolipoprotein A-IV	Apoa4	1.443	0.000
1451263_a_at	fatty acid binding protein 4, adipocyte	Fabp4	1.452	0.000
1423555_a_at	interferon-induced protein 44	Ifi44	1.539	0.000
1417023_a_at	fatty acid binding protein 4, adipocyte	Fabp4	1.554	0.000
1424775_at	2'-5' oligoadenylate synthetase 1A	Oas1a	1.564	0.000
1417185_at	lymphocyte antigen 6 complex, locus A	Ly6a	1.570	0.000
1450018_s_at	solute carrier family 25, member 30	Slc25a30	1.596	0.000

1417409_at	Jun oncogene	Jun	1.601	0.000
1419573_a_at	lectin, galactose binding, soluble 1	Lgals1	1.602	0.000
1460406_at	plastin 1 (I-isoform)	Pls1	1.613	0.000
1455439_a_at	lectin, galactose binding, soluble 1	Lgals1	1.622	0.001
1418486_at	vanin 1	Vnn1	1.630	0.005
1416930_at	lymphocyte antigen 6 complex, locus D	Ly6d	1.648	0.000
1427474_s_at	glutathione S-transferase, mu 3	Gstm3	1.683	0.001
1426278_at	interferon, alpha-inducible protein 27 like 2A	Ifi27l2a	1.721	0.000
1449153_at	matrix metallopeptidase 12	Mmp12	1.729	0.000
1420836_at	solute carrier family 25, member 30	Slc25a30	1.761	0.000
1418918_at	insulin-like growth factor binding protein 1	Igfbp1	1.904	0.005
1417256_at	matrix metallopeptidase 13	Mmp13	1.914	0.000
1452260_at	cell death-inducing DFFA-like effector c	Cidec	1.998	0.006
1419504_at	monoacylglycerol O-acyltransferase 1	Mogat1	2.158	0.002
1418191_at	ubiquitin specific peptidase 18	Usp18	2.182	0.000
1418712_at	CDC42 effector protein (Rho GTPase binding) 5	Cdc42ep5	2.224	0.000
1417017_at	cytochrome P450, family 17, subfamily a, polypeptide 1	Cyp17a1	2.631	0.001

Table 1. The list of the gene expression changes in the livers of SIRT7 KO mice compared to in the livers of WT control mice from the microarray analysis.

Gene Title	Gene Symbol	Fold Change	p Value
Growth Hormone Receptor	Ghr	-1.3	0.0019
Fibroblast Growth Factor 1	Fgf1	-1.58	0.0018
Epidermal Growth Factor Receptor	Egfr	-1.39	0.02
Fibroblast Growth Factor Receptor 4	Fgfr4	-1.87	4.16E-06
Prolactin Receptor	Prlr	-2.64	0.0009
IGF Binding Protein, Acid Labile	Igfals	-1.64	0.0003
IGF Binding Protein 3	Igfbp3	-2.16	0.04
IGF Binding Protein 1	Igfbp1	3.74	0.0048
IGF Binding Protein 7	Igfbp7	1.28	0.005
IGF Binding Protein 6	Igfbp6	1.19	0.04

Table 2. Differentially expressed genes related to the GH/IGF-1 signaling pathway in the livers of SIRT7 KO mice compared to in the livers of WT control mice from the microarray analysis.

Gene Title	Gene Symbol	Binding Region
IGF1 Receptor	IGF1R	Enhancer
IGF2 mRNA Binding Protein 1	IGF2BP1	Promoter/Enhancer
IGF2 mRNA Binding Protein 3	IGF2BP3	Promoter/Enhancer
IGF2 Receptor	IGF2R	Promoter/Enhancer
IGF Binding Protein 3	IGFBP3	Promoter/Enhancer
IGF Binding Protein 4	IGFBP4	Promoter/Enhancer
IGF Binding Protein 6	IGFBP6	Promoter/Enhancer
IGF Like Family Member 4	IGFL4	Promoter/Enhancer
IGF Like Family Receptor 1	IGFLR1	Enhancer

Table 3. A summary of IGF-related genes as ATF3 targets based on ChIP sequencing analysis using the Harmonizome web portal revealing ATF3 bindings to the promotors or enhancers of IGF-related genes.

References

[1] G. L. Imai S, Armstrong CM, Kaeberlein M, "Transcriptional silencing and longevity protein Sir2 is an NAD-dependent histone deacetylase," *Nature*, vol. 403, pp. 795–800, 2000.

[2] L. Bosch-Presegué and A. Vaquero, "Sirtuins in stress response: Guardians of the genome," *Oncogene*, vol. 33, no. 29. Nature Publishing Group, pp. 3764–3775, 17-Jul-2014.

[3] M. Mohrin *et al.*, "A mitochondrial UPR-mediated metabolic checkpoint regulates hematopoietic stem cell aging," *Science (80-.).*, vol. 347, no. 6228, pp. 1374–1377, 2015.

[4] J. Shin *et al.*, "SIRT7 represses myc activity to suppress er stress and prevent fatty liver disease," *Cell Rep.*, vol. 5, no. 3, pp. 654–665, 2013.

[5] D. Rudman, M. H. Kutner, C. M. Rogers, M. F. Lubin, G. A. Fleming, and R. P. Bain, "Impaired growth hormone secretion in the adult population. Relation to age and adiposity," *J. Clin. Invest.*, vol. 67, no. 5, pp. 1361–1369, 1981.

[6] L. J. Niedernhofer *et al.*, "A new progeroid syndrome reveals that genotoxic stress suppresses the somatotroph axis," *Nature*, vol. 444, no. 7122, pp. 1038–1043, Dec. 2006.

[7] M. P. Mattson and T. V. Arumugam, "Hallmarks of Brain Aging: Adaptive and Pathological Modification by Metabolic States," *Cell Metab.*, vol. 27, no. 6, pp. 1176–1199, 2018.

[8] D. J. Creer, C. Romberg, L. M. Saksida, H. Van Praag, and T. J. Bussey, "Running enhances spatial pattern separation in mice," *Proc. Natl. Acad. Sci. U. S. A.*, vol. 107, no. 5, pp. 2367–2372, Feb. 2010.

[9] F. A. Witte AV, Fobker M, Gellner R, Knecht S, "Caloric restriction improves memory in elderly humans," *PNAS*, vol. 106, no. 14, pp. 1225–60, 2009.

[10] F. C. Benedetta A, "Age-related cognitive decline: Can neural stem cells help us?," *Aging (Albany NY)*, vol. 4, pp. 176–186, 2012.

[11] M. F. Paredes *et al.*, "Does Adult Neurogenesis Persist in the Human Hippocampus?," *Cell Stem Cell*, vol. 23, no. 6. Cell Press, pp. 780–781, 06-Dec-2018.

[12] L. O. 12. Tobin MK, Musaraca K, Disouky A, Shetti A, Bheri A, Honer WG, Kim N, Dawe RJ, Bennett DA, Arfanakis K, "Human Hippocampal Neurogenesis Persists in Aged Adults and Alzheimer's Disease Patients," *Cell Stem Cell*, vol. 24, pp. 974–982, 2019.

[13] J. Altman, "Autoradiographic and Histological Studies of Postnatal Neurogenesis IV. CELL PROLIFERATION AND MIGRATION IN THE ANTERIOR FOREBRAIN, WITH SPECIAL REFER-ENCE TO PERSISTING NEUROGENESIS IN THE OLFACTORY BULB," *J Comp Neurol*, vol. 137, pp. 433–457, 1969.

[14] A.-B. A. Lois C, "Long-distance neuronal migration in the adult mammalian brain," *Science (80-.).*, vol. 264, pp. 1145–1148, 1994.

[15] A. Alvarez-Buylla and J. Manuel García-Verdugo, "Neurogenesis in Adult Subventricular Zone," 2002.

[16] H. J. Kaplan MS, “Neurogenesis in the adult rat: electron microscopic analysis of light radioautographs,” *Science (80-.).*, vol. 197, pp. 1092–1094, 1977.

[17] H. A. Cameron, C. S. Woolley, B. S. Mcewen, and E. Gould, “DIFFERENTIATION OF NEWLY BORN NEURONS AND GLIA IN THE DEBATE GYRUS OF THE ADULT RAT,” 1993.

[18] C. Rochefort, G. Gheusi, J.-D. Vincent, and P.-M. Lledo, “Enriched Odor Exposure Increases the Number of Newborn Neurons in the Adult Olfactory Bulb and Improves Odor Memory,” 2002.

[19] R. Belvindrah, S. Hankel, J. Walker, B. L. Patton, and U. Müller, “β1 integrins control the formation of cell chains in the adult rostral migratory stream,” *J. Neurosci.*, vol. 27, no. 10, pp. 2704–2717, Mar. 2007.

[20] K. Sawamoto *et al.*, “Cellular composition and organization of the subventricular zone and rostral migratory stream in the adult and neonatal common marmoset brain,” *J. Comp. Neurol.*, vol. 519, no. 4, pp. 690–713, Mar. 2011.

[21] C. Wang *et al.*, “Identification and characterization of neuroblasts in the subventricular zone and rostral migratory stream of the adult human brain,” *Cell Res.*, vol. 21, no. 11, pp. 1534–1550, Nov. 2011.

[22] A. Arvidsson, T. Collin, D. Kirik, Z. Kokaia, and O. Lindvall, “Neuronal replacement from endogenous precursors in the adult brain after stroke,” *Nat. Med.*, vol. 8, no. 9, pp. 963–970, 2002.

[23] J. M. Parent, Z. S. Vexler, C. Gong, N. Derugin, and D. M. Ferriero, “Rat Forebrain Neurogenesis and Striatal Neuron Replacement after Focal Stroke,” 2002.

[24] T. Yamashita *et al.*, “Subventricular zone-derived neuroblasts migrate and differentiate into mature neurons in the post-stroke adult striatum,” *J. Neurosci.*, vol. 26, no. 24, pp. 6627–6636, 2006.

[25] G. E. Goings, V. Sahni, and F. G. Szele, “Migration patterns of subventricular zonecells in adult mice change after cerebral cortex injury,” *Brain Res.*, vol. 996, no. 2, pp. 213–226, Jan. 2004.

[26] J. T. Gonçalves, S. T. Schafer, and F. H. Gage, “Adult Neurogenesis in the Hippocampus: From Stem Cells to Behavior,” *Cell*, vol. 167, no. 4. Cell Press, pp. 897–914, 03-Nov-2016.

[27] N. Kee, C. M. Teixeira, A. H. Wang, and P. W. Frankland, “Preferential incorporation of adult-generated granule cells into spatial memory networks in the dentate gyrus,” *Nat. Neurosci.*, vol. 10, no. 3, pp. 355–362, Mar. 2007.

[28] V. Ramirez-Amaya, D. F. Marrone, F. H. Gage, P. F. Worley, and C. A. Barnes, “Integration of new neurons into functional neural networks,” *J. Neurosci.*, vol. 26, no. 47, pp. 12237–12241, Nov. 2006.

[29] R. G. Bechara and á M. Kelly, “Exercise improves object recognition memory and induces BDNF expression and cell proliferation in cognitively enriched rats,” *Behav. Brain Res.*, vol. 245, pp. 96–100, May 2013.

[30] A. K. E. Hornsby *et al.*, “Short-term calorie restriction enhances adult hippocampal neurogenesis and remote fear memory in a Ghsr-dependent manner,” *Psychoneuroendocrinology*, vol. 63, pp. 198–207, Jan. 2016.

[31] T. Qu, C. L. Brannen, H. M. Kim, and K. Sugaya, “Human neural stem cells improve cognitive function of aged brain,” *Lippincott Williams & Wilkins*, vol. 12, no. 6, 2001.

[32] R. L. Katsimpardi L, Litterman NK, Schein PA, Miller CM, Loffredo FS, Wojtkiewicz GR, Chen JW, Lee RT, Wagers AJ, “Vascular and Neurogenic Rejuvenation of the Aging Mouse Brain by Young Systemic Factors,” *Science (80-.).*, vol. 344, no. 6184, pp. 630–634, 2014.

[33] J. M. Castellano *et al.*, “Human umbilical cord plasma proteins revitalize hippocampal function in aged mice,” *Nature*, vol. 544, no. 7651, pp. 488–492, 2017.

[34] C. B. Johansson, M. Svensson, L. Wallstedt, A. M. Janson, and J. Frisén,“RAPID COMMUNICATION Neural Stem Cells in the Adult Human Brain,” 1999.

[35] G. Rushing and R. A. Ihrie, “Neural stem cell heterogeneity through time and space in the ventricular-subventricular zone,” *Frontiers in Biology*, vol. 11, no. 4. Higher Education Press, pp. 261–284, 01-Aug-2016.

[36] Z. Chaker, P. Codega, and F. Doetsch, “A mosaic world: puzzles revealed by adult neural stem cell heterogeneity,” *Wiley Interdisciplinary Reviews: Developmental Biology*, vol. 5, no. 6. John Wiley and Sons Inc., pp. 640–658, 01-Nov-2016.

[37] J. Y. Kim, M. R. Shaker, J. H. Lee, B. Lee, H. Kim, and W. Sun, “Identification of molecular markers distinguishing adult neural stem cells in the subventricular and subcallosal zones,” *Animal Cells Syst. (Seoul).*, vol. 21, no. 3, pp. 152–159, May 2017.

[38] H. Song, D. A. Berg, A. M. Bond, and G. li Ming, “Radial glial cells in the adult dentate gyrus: What are they and where do they come from?,” *F1000Research*, vol. 7. Faculty of 1000 Ltd, 2018.

[39] W. S. Reynolds BA, “Generation of neurons and astrocytes from isolated cells of the adult mammalian central nervous system,” *Science (80-.).*, vol. 255, pp. 1707–10, 1992.

[40] R. B. Louis SA, “Generation and Differentiation of Neurospheres From Murine Embryonic Day 14 Central Nervous System Tissue,” *Method Mol. Biol.*, vol. 290, pp. 265–280, 2009.

[41] E. Navarro Quiroz *et al.*, “Cell Signaling in Neuronal Stem Cells,” *Cells*, vol. 7, no. 7, p. 75, Jul. 2018.

[42] S. Artavanis-Tsakonas, M. D. Rand, and R. J. Lake, “Notch Signaling: Cell Fate Control and Signal Integration in Development.”

[43] U. Marklund *et al.*, “Domain-specific control of neurogenesis achieved through patterned regulation of Notch ligand expression,” *Development*, vol. 137, no. 3, pp. 437–445, Feb. 2010.

[44] A. Matsumoto, I. Onoyama, T. Sunabori, R. Kageyama, H. Okano, and K. I. Nakayama, “Fbxw7-dependent degradation of notch is required for control of ‘Stemness’ and neuronal-glial differentiation in neural stem cells,” *J. Biol. Chem.*, vol. 286, no. 15, pp.

13754–13764, 2011.

[45] S. D. Calvi LM, Adams GB, Weibrecht KW, Weber JM, Olson DP, Knight MC, Martin RP, Schipani E, Divieti P, Bringhurst FR, Milner LA, Kronenberg HM, "Osteoblastic cells regulate the haematopoietic stem cell niche," *Nature*, vol. 425, no. 6960, pp. 841–6, Oct. 2003.

[46] A. W. Duncan *et al.*, "Integration of Notch and Wnt signaling in hematopoietic stem cell maintenance," *Nat. Immunol.*, vol. 6, no. 3, pp. 314–322, 2005.

[47] L. A. Milner, R. Kopan, D. I. K. Martin, and I. D. Bernstein, "A Human Homologue of the Drosophila Developmental Gene, Notch, Is Expressed in CD34+ Hematopoietic Precursors."

[48] R. Kopan and M. X. G. Ilagan, "The Canonical Notch Signaling Pathway: Unfolding the Activation Mechanism," *Cell*, vol. 137, no. 2. pp. 216–233, 17-Apr-2009.

[49] J. Hatakeyama *et al.*, "Hes genes regulate size, shape and histogenesis of the nervous system by control of the timing of neural stem cell differentiation," *Development*, vol. 131, no. 22, pp. 5539–5550, Nov. 2004.

[50] I. Imayoshi, M. Sakamoto, M. Yamaguchi, K. Mori, and R. Kageyama, "Essential roles of Notch signaling in maintenance of neural stem cells in developing and adult brains," *J. Neurosci.*, vol. 30, no. 9, pp. 3489–3498, Mar. 2010.

[51] L. Grandbarbe, J. Bouissac, M. Rand, M. Hrabé de Angelis, S. Artavanis-Tsakonas, and E. Mohier, "Delta-Notch signaling controls the generation of neurons/glia from neural stem cells in a stepwise process," *Development*, vol. 130, no. 7. pp. 1391–1402, Apr-2003.

[52] S. J. Morrison *et al.*, "Transient Notch Activation Initiates an Irreversible Switch from Neurogenesis to Gliogenesis by Neural Crest Stem Cells stem cells (NCSCs) self-renew and can generate one or more classes of neurons, glia, and myofibroblasts (also known as smooth muscle cells) in vitro (Stemple and Anderson, 1992). Moreover, the fate of NCSCs can be controlled by instructive extracellular signals such as," 2000.

[53] I. Ackers and R. Malgor, "Interrelationship of canonical and non-canonical Wnt signalling pathways in chronic metabolic diseases," *Diabetes and Vascular Disease Research*, vol. 15, no. 1. SAGE Publications Ltd, pp. 3–13, 01-Jan-2018.

[54] B. T. MacDonald, K. Tamai, and X. He, "Wnt/β-Catenin Signaling: Components, Mechanisms, and Diseases," *Developmental Cell*, vol. 17, no. 1. pp. 9–26, 21-Jul-2009.

[55] H. R. Komiya Y, "Wnt Secretion and Extra-Cellular Regulators," *Organogenesis*, vol. 4, pp. 68–75, 2008.

[56] S. Angers and R. T. Moon, "Proximal events in Wnt signal transduction," *Nature Reviews Molecular Cell Biology*, vol. 10, no. 7. pp. 468–477, Jul-2009.

[57] N. Bengoa-Vergniory and R. M. Kypta, "Canonical and noncanonical Wnt signaling in neural stem/progenitor cells," *Cellular and Molecular Life Sciences*, vol. 72, no. 21. Birkhauser Verlag AG, pp. 4157–4172, 01-Nov-2015.

[58] D. C. Lie *et al.*, "Wnt signalling regulates adult hippocampal neurogenesis," *Nature*, vol. 437, no. 7063, pp. 1370–1375, Oct. 2005.

[59] K. T. Okamoto M, Inoue K, Iwamura H, Terashima K, Soya H, Asashima M, “Reduction in paracrine Wnt3 factors during aging causes impaired adult neurogenesis,” *FASEB J*, vol. 25, pp. 3570–82, 2011.

[60] M. Chen and H. Do, “Wnt signaling in neurogenesis during aging and physical activity,” *Brain Sci.*, vol. 2, no. 4, pp. 745–768, 2012.

[61] L. Varela-Nallar, I. E. Alfaro, F. G. Serrano, J. Parodi, and N. C. Inestrosa,“Wingless-type family member 5A (Wnt-5a) stimulates synaptic differentiation and function of glutamatergic synapses,” *Proc. Natl. Acad. Sci. U. S. A.*, vol. 107, no. 49, pp. 21164–21169, Dec. 2010.

[62] L. Ciani *et al.*, “Wnt7a signaling promotes dendritic spine growth and synaptic strength through Ca 2+/Calmodulin-dependent protein kinase II,” *Proc. Natl. Acad. Sci. U. S. A.*, vol. 108, no. 26, pp. 10732–10737, Jun. 2011.

[63] V. Tropepe, M. Sibilia, B. G. Ciruna, J. Rossant, E. F. Wagner, and D. Van Der Kooy, “Distinct Neural Stem Cells Proliferate in Response to EGF and FGF in the Developing Mouse Telencephalon,” 1999.

[64] B. A. Reynolds and S. Weiss, “Clonal and Population Analyses Demonstrate That an EGF-Responsive Mammalian Embryonic CNS Precursor Is a Stem Cell,” 1996.

[65] Y. Arsenijevic, S. Weiss, B. Schneider, and P. Aebischer, “Insulin-Like Growth Factor-I Is Necessary for Neural Stem Cell Proliferation and Demonstrates Distinct Actions of Epidermal Growth Factor and Fibroblast Growth Factor-2 is a potent tool for delineating the actions of epige-netic and intrinsic factors on precursors for neurons (Ahmed et al Control of NSC proliferation depends on the ac-tions of epidermal growth factor (EGF) and/or its homolog transforming growth factor-, basic fibroblast growth factor (FGF-2), and the p75 receptor (Reynolds et al,” Arsenijevic and Weiss, 1992.

[66] L. H. Hu JG, Zhang YX, Qi Q, Wang R, Shen L, Zhang C, Xi J, Zhou JS, “Expression of BMP-2 and BMP-4 proteins by type-1 and type-2 astrocytes induced from neural stem cells under different differentiation conditions,” *Acta Neurobiol Exp*, vol. 72, pp. 95–101, 2012.

[67] A. M. Bond, O. G. Bhalala, and J. A. Kessler, “The dynamic role of bone morphogenetic proteins in neural stem cell fate and maturation,” *Dev. Neurobiol.*, vol. 72, no. 7, pp. 1068–1084, Jul. 2012.

[68] T. Taga and S. Fukuda, “IL-6 in Neural Stem Cell Differentiation Role of IL-6 in the Neural Stem Cell Differentiation,” 2005.

[69] T. Zigova, V. Pencea, S. J. Wiegand, and M. B. Luskin, “Intraventricular Administration of BDNF Increases the Number of Newly Generated Neurons in the Adult Olfactory Bulb,” 1998.

[70] A. Benraiss, E. Chmielnicki, K. Lerner, D. Roh, and S. A. Goldman, “Adenoviral Brain-Derived Neurotrophic Factor Induces Both Neostriatal and Olfactory Neuronal Recruitment from Endogenous Progenitor Cells in the Adult Forebrain,” 2001.

[71] V. Pencea, K. D. Bingaman, S. J. Wiegand, and M. B. Luskin, “Infusion of Brain-Derived Neurotrophic Factor into the Lateral Ventricle of the Adult Rat Leads to New Neurons in

the Parenchyma of the Striatum, Septum, Thalamus, and Hypothalamus," 2001.

[72] S. A. Villeda *et al.*, "The ageing systemic milieu negatively regulates neurogenesis and cognitive function," *Nature*, vol. 477, no. 7362, pp. 90–96, Sep. 2011.

[73] J. Walter, S. Keiner, O. W. Witte, and C. Redecker, "Age-related effects on hippocampal precursor cell subpopulations and neurogenesis," *Neurobiol. Aging*, vol. 32, no. 10, pp. 1906–1914, Oct. 2011.

[74] J. M. Encinas *et al.*, "Division-coupled astrocytic differentiation and age-related depletion of neural stem cells in the adult hippocampus," *Cell Stem Cell*, vol. 8, no. 5, pp. 566–579, May 2011.

[75] D. S. Leeman *et al.*, "Lysosome activation clears aggregates and enhances quiescent neural stem cell activation during aging."

[76] C. Franceschi and J. Campisi, "Chronic inflammation (Inflammaging) and its potential contribution to age-associated diseases," *Journals of Gerontology - Series A Biological Sciences and Medical Sciences*, vol. 69. Oxford University Press, pp. S4–S9, 01-Jun-2014.

[77] P. T. Monje ML, Toda H, "Inflammatory blockade restores adult hippocampal neurogenesis," *Science (80-.).*, vol. 302, pp. 1760–5, 2003.

[78] I. Goshen and R. Yirmiya, "Interleukin-1 (IL-1): A central regulator of stress responses," *Frontiers in Neuroendocrinology*, vol. 30, no. 1. pp. 30–45, Jan-2009.

[79] M. E. Woodbury *et al.*, "miR-155 is essential for inflammation-induced hippocampal neurogenic dysfunction," *J. Neurosci.*, vol. 35, no. 26, pp. 9764–9781, Jul. 2015.

[80] M. D. Wu, A. M. Hein, M. J. Moravan, S. S. Shaftel, J. A. Olschowka, and M. K. O'Banion, "Adult murine hippocampal neurogenesis is inhibited by sustained IL-1β and not rescued by voluntary running," *Brain. Behav. Immun.*, vol. 26, no. 2, pp. 292–300, Feb. 2012.

[81] T. D. P. Michelle L. Monje, Hiroki Toda, "Inflammatory Blockade Restores Adult Hippocampal Neurogenesis," vol. 302, no. December, pp. 1760–1765, 2003.

[82] L. Fontana, L. Partridge, and V. D. Longo, "Extending Healthy Life Span-From Yeast to Humans."

[83] A. Bartke, "Growth Hormone and Aging: Updated Review," *World J. Mens. Health*, vol. 37, no. 1, p. 19, 2019.

[84] A. Gesing *et al.*, "A Long-lived Mouse Lacking Both Growth Hormone and Growth Hormone Receptor: A New Animal Model for Aging Studies," *Journals Gerontol. - Ser. A Biol. Sci. Med. Sci.*, vol. 72, no. 8, pp. 1054–1061, Aug. 2017.

[85] C. G. Tsigos C, Kyrou I, Kassi E, "Stress, Endocrine Physiology and Pathophysiology," in *Endotext*, 2000.

[86] Z. Laron, "Insulin-like growth factor 1 (IGF-1): A growth hormone," *J. Clin. Pathol. - Mol. Pathol.*, vol. 54, no. 5, pp. 311–316, 2001.

[87] R. D. Kineman, M. del Rio-Moreno, and A. Sarmento-Cabral, "40 years of IGF1: Understanding the tissue-specific roles of IGF1/IGF1R in regulating metabolism using the

Cre/loxP system," *Journal of Molecular Endocrinology*, vol. 61, no. 1. BioScientifica Ltd., pp. T187–T198, 01-Jul-2018.

[88] N. M. Ashpole *et al.*, "IGF-1 has sexually dimorphic, pleiotropic, and time-dependent effects on healthspan, pathology, and lifespan," *GeroScience*, vol. 39, no. 2, pp. 129–145, Apr. 2017.

[89] G. Vitale, G. Pellegrino, M. Vollery, and L. J. Hofland, "ROLE of IGF-1 System in the Modulation of Longevity: Controversies and New Insights From a Centenarians' Perspective," *Front. Endocrinol. (Lausanne).*, vol. 10, Feb. 2019.

[90] C. J. Reddy SSK, "The Endocrinology of aging: a key to longevity "Great Expectations"," *Endocr Pr.*, vol. 23, pp. 1107–16, 2017.

[91] R. K. Junnila, E. O. List, D. E. Berryman, J. W. Murrey, and J. J. Kopchick, "The GH/IGF-1 axis in ageing and longevity," *Nature Reviews Endocrinology*, vol. 9, no. 6. pp. 366–376, Jun-2013.

[92] S. Milman *et al.*, "Low insulin-like growth factor-1 level predicts survival in humans with exceptional longevity," *Aging Cell*, vol. 13, no. 4, pp. 769–771, 2014.

[93] van der L. A. Lamberts SW, van den Beld AW, "The endocrinology of aging," 1997.

[94] T. Doi *et al.*, "Association of insulin-like growth factor-1 with mild cognitive impairment and slow gait speed," *Neurobiol. Aging*, vol. 36, no. 2, pp. 942–947, Feb. 2015.

[95] C. V. Vorhees and M. T. Williams, "Morris water maze: Procedures for assessing spatial and related forms of learning and memory," *Nat. Protoc.*, vol. 1, no. 2, pp. 848–858, 2006.

[96] G. A. Garinis *et al.*, "Persistent transcription-blocking DNA lesions trigger somatic growth attenuation associated with longevity," *Nat. Cell Biol.*, vol. 11, no. 5, pp. 604–615, 2009.

[97] M. K. Brown and N. Naidoo, "The endoplasmic reticulum stress response in aging and age-related diseases," *Frontiers in Physiology*, vol. 3 JUL. 2012.

[98] W. Yan *et al.*, " Arginine methylation of SIRT 7 couples glucose sensing with mitochondria biogenesis ," *EMBO Rep.*, vol. 19, no. 12, pp. 1–15, 2018.

[99] J. B. Allard and C. Duan, "IGF-binding proteins: Why do they exist and why are there so many?," *Front. Endocrinol. (Lausanne).*, vol. 9, no. APR, pp. 1–12, 2018.

[100] B. N. Vazquez *et al.*, " SIRT 7 promotes genome integrity and modulates non-homologous end joining DNA repair ," *EMBO J.*, vol. 35, no. 14, pp. 1488–1503, 2016.

[101] H. Y. Seo *et al.*, "Endoplasmic reticulum stress-induced activation of activating transcription factor 6 decreases cAMP-stimulated hepatic gluconeogenesis via inhibition of CREB," *Endocrinology*, vol. 151, no. 2, pp. 561–568, 2010.

[102] S. P. Persengiev and M. R. Green, "The role of ATF/CREB family members in cell growth, survival and apoptosis," *Apoptosis*, vol. 8, no. 3, pp. 225–228, 2003.

[103] M. E. Fusakio *et al.*, "Transcription factor ATF4 directs basal and stress-induced gene expression in the unfolded protein response and cholesterol metabolism in the liver," *Mol. Biol. Cell*, vol. 27, no. 9, pp. 1536–1551, 2016.

[104] C. J. Fiorese, A. M. Schulz, Y. F. Lin, N. Rosin, M. W. Pellegrino, and C. M. Haynes, "The Transcription Factor ATF5 Mediates a Mammalian Mitochondrial UPR," *Curr. Biol.*, vol. 26, no. 15, pp. 2037–2043, 2016.

[105] Y. Tanaka *et al.*, "Systems analysis of ATF3 in stress response and cancer reveals opposing effects on pro-apoptotic genes in p53 pathway," *PLoS One*, vol. 6, no. 10, 2011.

Appendix: Materials and Methods

Mice

SIRT7-/- mice have been described previously [3,4]. All mice were housed on a 12:12 hr light:dark cycle at 25°C. All animal procedures were in accordance with the animal care committee at the University of California, Berkeley. Oxygen consumption was measured with the Oxymax-Comprehensive Laboratory Animal Monitoring System (Columbus Instruments) for 2 days. Mice were fasted for the first day and fed for the second day.

Immunohistochemistry

Tissue processing and immunohistochemistry was performed on free-floating sections. Briefly, mice were transcardially perfused with 10 ml of PBS with 10 U/ml of heparin and then with 40 ml of PBS with 4% formaldehyde. Brains were extracted and incubated in PBS with 4% formaldehyde at 4℃ for a day. The brains were transferred into PBS with 15% at 4℃ for 6 hr and then transferred into PBS with 30% at 4℃ for a day before cutting. Brains were then sectioned coronally at 40 μm with a cryomicrotome (Leica Camera, Inc.) and stored in cryoprotective medium. The brain sections were pre-treated with 2N HCl at 37°C for 30 min before incubation with primary antibody. Primary antibodies were: mouse anti-Dcx (1:200; Santa Cruz), rat anti-BrdU (1:5000, Invitrogen), goat anti-Sox2 (5ug/ml, Biolegend), mouse anti-NeuN (1:500, Millipore) and rabbit anti-S100β (1:1500, Biolegend). After overnight incubation, primary antibody staining was revealed using TSA plus biotin kit (PerkinElmer) or fluorescence conjugated secondary antibodies. To estimate the total number of Dcx or Sox2 positive cells per DG immunopositive cells in the granule cell and subgranular cell layer of the DG were counted in every sixth coronal hemibrain section through the hippocampus and multiplied by 12.

BrdU experiments

For a 1-day BrdU experiment, mice were given 1 intraperitoneal injection of BrdU (50 mg/kg body weight) per day for 3 days and euthanized 24hr after the final injection. For a 4-weeks BrdU experiment, mice were given 1 intraperitoneal injection of BrdU (50 mg/kg body weight) per day for 5 days and euthanized 28 days after the final injection.

Morris Water Maze

Mice were trained on the MWM [95] with four trials per day over 5 to 7 days. The tank diameter was 122cm and the platform was hidden 1 cm below the surface of water made opaque with white nontoxic paint. Starting points were changed every day. Each trial lasted either until the mouse found the platform or for 60 seconds. Mice rested on the platform for 10 seconds after each trial. 24 hours and 72 hours after the last training session on day 5 or 7, the platform was removed for a 60 seconds probe trial. Swim path length and speed were recorded (Ethovision; Noldus Information Technology, Wageningen, The Netherlands).

Affymetrix microarray and pathway analysis

Total RNA was isolated from the livers of wild type and SIRT7-/- mice using an RNA isolation kit (Qiagen). Microarray hybridizations were performed at the University of California, Berkeley Functional Genomics Laboratory using Affymetrix GeneChip mouse 430As according to the instructions of the manufacturer (Affymetrix). RMA normalization was applied and the limma packagewas used to identify the differentially expressed genes. Differentially expressed genes were selected using the Benjamini-Hochberg method to control the FDR at 15%. DAVID v6.8 (https://david.ncifcrf.gov/) was used to find significantly enriched KEGG pathways and gene ontology (GO) terms.

Quantitative Real-Time PCR

RNA was isolated from cells or tissues using Trizol reagent (Invitrogen) following the manufacturer's instructions. cDNA was generated using the qScript cDNA SuperMix (Quanta Biosciences). Gene expression was determined by quantitative real time PCR using Eva qPCR SuperMix kit (BioChain Institute) on an ABI StepOnePlus system. All data were normalized to GAPDH expression.

AAV8-mediated gene transfer

For AAV8-mediated gene transfer to the mouse liver, SIRT7 or Myc knockdown target sequence was cloned into dsAAV-RSVeGFP-U6 vector. AAV8 for overexpressing SIRT7 or knocking down Myc was produced by Vigene biosciences. AAV8 for knocking down ATF3 was acquired from Vector biolabs. Myc knockdown target sequence: 5'-CCCAAGGTAGTGATCCTCAAA-3'. ATF3 knockdown target sequence: 5'-TGCTGCCAAGTGTCGAAACAA-3'. Each mouse was injected with 3×10^{11} genome copies of virus via tail vein. Mice were characterized four weeks after viral infection.

IGF1 level

To detect free IGF-1 in plasma, the plasma was pretreated with acid-ethanol extraction solution and plasma IGF-1 was detected using IGF-1 Mouse ELISA Kit (Invitrogen).

Statistical Analysis

Mice were randomized to groups and analysis of mice and tissue samples was performed by investigators blinded to the treatment or the genetic background of the animals. Statistical analysis was performed with t test (Excel). The statistic of MWM was performed with t-test or 2-way ANOVA (prism). The statistic of gene length analysis was performed with two-way ANOVA (Excel). Data are presented as means and error bars represent standard errors. In all corresponding figures, * represents $p < 0.05$. ** represents $p < 0.01$. *** represents $p < 0.001$. ns represents $p > 0.05$. Replicate information is indicated in the figures.

Antibodies	Source	Catalog #
BrdU	Invitrogen	MA1-82088
Sox2	Biolegend	651902
Dcx	Santacruz	OASG02231
NeuN	Millipore	MAB377
S100β	Invitrogen	701340
p-eIF2α	Invitrogen	44728G
p-Akt (Ser473)	CST	9271
p-Akt (Thr308)	CST	9275
Akt	CST	9272
Actin	Sigma	A2066

Antibodies used in this study

Gene	Primer	Sequence
GAPDH	Forward	ACCCAGAAGACTGTGGATGG
	Reverse	ACACATTGGGGGTAGGAACA
GHR	Forward	ATTCACCAAGTGTCGTTCC
	Reverse	TCCATTCCTGGGTCCATTCA
FGF1	Forward	GGCCAGAAAGCCATCTCGTTT
	Reverse	TAGCGCAGCCAATGGTCAA
EGFR	Forward	GGAAACCGAAATTTGTGCTACG
	Reverse	GCCTTGCAGTCTTTCTCAGCTC
FGFR4	Forward	GGCTATGCTGTGGCCGCACT
	Reverse	GGTCTGAGGGCACCACGCTC
IGFBP1	Forward	TCGCCGACCTCAAGAAATGG
	Reverse	GGATGTCTCACACTGTTTGCT
IGF-1	Forward	TGCTTGCTCACCTTCACCA
	Reverse	CAACACTCATCCACAATGCC
IGFBP3	Forward	AACATCAGTGAGTCCGAGG
	Reverse	AACTTTGTAGCGCTGGCTG
IGF-1R	Forward	ACGACAACACAACCTGCGT
	Reverse	AACGAAGCCATCCGAGTCA
ATF3	Forward	AGCCTGGAGCAAAATGATGCTT
	Reverse	AGGTTAGCAAAATCCTCAAACAC

Primer sequences for qPCR used in this study